Hyperbionic Reading:
A Visual Projection of Prosodic Parameter Space

Flyxion

Independent Researcher

Abstract

Written language is a lossy projection of speech that preserves lexical structure while discarding prosody, timing, and spatial acoustics. This essay proposes Hyperbionic Reading as a formal system that restores these lost dimensions by embedding prosodic invariants directly into the visual properties of typography. We establish that acoustic analysis, modal resonance storage, and Hyperbionic rendering are not merely analogous but equivalent as parameterized projections of a shared invariant structure: the prosodic parameter vector extracted from a waveform by peak-derived measurement. This equivalence extends to higher-dimensional acoustic features—delay and reverberation—which admit precise typographic operators. The analysis is further extended into the temporal domain, where spoken words are treated not as static points in feature space but as trajectories through a modal lattice, yielding a wave-native architecture for speech recognition as trajectory resonance. The culminating claim is that marked-up text is not decorated language but a higher-dimensional prosodic encoding, and that Hyperbionic Reading is the visual projection of the same invariant structure that acoustic analysis measures and resonant memory stores.

Orientation

The following exposition develops the theoretical foundations of Hyperbionic Reading as a system for restoring prosodic structure to written language. The central claim is that prosody is not an ancillary feature of speech but a measurable, invariant structure that admits consistent representation across acoustic, geometric, and visual domains. This document should be read as the construction of a single invariant object viewed through multiple coordinate systems. The acoustic waveform, the modal lattice coordinate, and the Hyperbionic rendering are not independent representations but projections of a shared prosodic field. The purpose of the exposition is therefore not to introduce separate techniques but to show that these apparently distinct operations commute: measurement, storage, and rendering preserve the same structure under change of medium. Each section re-establishes the invariant before developing the next layer of the pipeline.

A note on presentation: the paper applies its own rendering operator to itself. Invariant identities, ontological pivots, and structural definitions are rendered at elevated visual energy (larger, bolder type), corresponding to high values of e_i and s_i in the Hyperbionic parameter space. This is not stylistic decoration but a proof of concept: the same emphasis logic that the theory describes is instantiated in the typography of the document.

Introduction: Text as Lossy Projection

When speech is transcribed into writing, the resulting symbol sequence preserves very little of the original signal. Lexical content survives—the identity of words, their grammatical arrangement—but the continuous structure that carries a large fraction of communicative meaning does not. Pitch contour, amplitude envelope, temporal rhythm, the degree of periodicity in voiced sounds, the spatial diffusion of reverberation: none of these are recoverable from a plain text string. The information they carry—emotional valence, prosodic emphasis, the speaker's certainty or hesitation, the acoustic properties of the environment—is simply absent.

This is not an incidental limitation of writing systems. It is a structural consequence of reducing a high-dimensional continuous signal to a sequence of discrete categorical tokens. The question this essay addresses is whether that reduction is necessary, or whether typography can be extended into a system that preserves prosodic structure by distributing it across the visual degrees of freedom that rendered text already possesses but does not exploit: size, weight, baseline position, spacing, rotation, opacity, blur, layering.

The answer developed here is that such an extension is not merely possible but formally well-defined. What is required is not an augmentation of text but a reconstruction of the signal pathway that was collapsed during transcription. This pathway consists of three operators: a measurement operator $\mathcal{M}$ that extracts prosodic invariants from sound, a storage operator Q that preserves those invariants geometrically, and a rendering operator R that re-expresses them in a visual medium. **Hyperbionic Reading is not decorated text. It is a projection of prosodic signal into visual space.** The extension requires three things: a compact representation of the prosodic structure of an acoustic signal, an operator that maps that representation into visual parameters, and a notion of equivalence across the acoustic, stored, and visual forms of the same prosodic information. Each of these is developed in turn.

Positioning: From Bionic Reading to Hyperbionic Reading

This section situates the present framework relative to existing work on enhanced reading, establishing that Hyperbionic Reading is not an optimization of existing text-presentation methods but a category shift from decoding acceleration to signal reconstruction.

Bionic Reading, developed by Renato Casutt, bolds the initial letters of words to create artificial fixation points. The rationale is well-grounded in reading science: fluent reading is not a serial decoding of characters but a predictive pattern-matching process in which partial orthographic cues activate learned letter-cluster patterns (bigrams, trigrams), and the brain completes the recognition from those seeds. By amplifying the initial n-gram signal, Bionic Reading gives the predictive system a stronger activation cue, potentially accelerating word recognition for some readers.

This is correct as far as it goes. The mechanism it exploits is real, and its benefits for readers with ADHD or dyslexia have been documented. But the scope of the claim is narrow: Bionic Reading optimizes lexical recognition speed within the symbolic register. Its implicit model of reading is

$$\text{meaning} \approx \text{lexical recognition speed}, \tag{1}$$

which is a very restricted slice of what reading actually involves. It does not encode prosody, emotional valence, temporal structure, ambiguity resolution, or context. It helps a reader recognize words faster; it does not help a reader understand why those words were said in a particular way, with what physical tension, at what speed, or in what acoustic environment.

The contrast with the present framework can be stated cleanly. Bionic Reading works *within* plain text by providing better triggers for the brain's prediction mechanism; Hyperbionic Reading works *beyond* plain text by restoring dimensions of signal that symbolic transcription discarded. The difference is:

$$\underbrace{\text{Bionic Reading}}_{\text{optimized decoding}} \longrightarrow \text{faster recognition of the same information.} \tag{2}$$

$$\underbrace{\text{Hyperbionic Reading}}_{\text{signal reconstruction}} \longrightarrow \text{recovery of information that was structurally absent.} \tag{3}$$

This is a category difference, not a degree difference. Bionic Reading assumes that the information needed to understand is already in the text and needs only to be accessed more efficiently. Hyperbionic Reading assumes that the information needed to understand was never in the text and must be projected back in from the acoustic signal.

The N-gram Connection and Its Extension

The n-gram intuition underlying Bionic Reading generalizes in a direction that connects directly to the present framework. Bionic Reading exploits the fact that word recognition is prediction from partial cues: given the first three letters of a seven-letter word, a fluent reader's brain completes the pattern. The signal is sparse; the prediction fills the gap.

Hyperbionic Reading applies the same principle at a higher level. Where Bionic Reading strengthens the prefix cue for *lexical* prediction, Hyperbionic Reading encodes the full trajectory of the *prosodic* signal. Instead of helping the brain predict which word follows which letters, it gives the brain the temporal and tonal structure that allows it to reconstruct the meaning of how words were spoken. The formal analogue is:

$$\text{Bionic Reading:} \quad \text{word} \approx \text{prefix cue} + \text{prediction}, \tag{4}$$

$$\text{Hyperbionic Reading:} \quad \text{meaning} = (\text{location, curvature, coherence}). \tag{5}$$

Bionic Reading compresses text into better triggers for the brain's internal reconstruction. Hyperbionic Reading encodes the signal directly so that the brain does not need to guess.

Why Listening-Based Learning Connects

This framework also clarifies an empirically observed phenomenon in language acquisition: a learner who hears a language extensively, without explicit grammar instruction, often develops fluency faster than one who studies rules. The standard explanation appeals to statistical learning of phonological patterns. The present framework offers a more precise account: extensive listening builds a trajectory space of speech patterns. The learner internalises not just which words follow which words, but the timing, stress, amplitude modulation, and jitter profiles that distinguish register, emotion, and pragmatic function. They learn the geometry of language in the modal parameter space $V = (\mathbb{R}^8, G)$, not merely its symbolic surface.

When such a learner encounters text, they are performing a reconstruction:

$$\text{text} \;\to\; \text{reconstruction of known trajectories from symbol cues.} \tag{6}$$

Bionic Reading improves the symbol cues that trigger this reconstruction (better prefix seeds). Hyperbionic Reading removes the need for internal reconstruction by encoding the trajectory directly in the text:

$$\text{Hyperbionic text} \;\to\; \text{direct presentation of the trajectory.} \tag{7}$$

A reader with a rich trajectory space from extensive listening has good internal models to fill in what Bionic Reading leaves implicit. A reader without that internal space—including a new language learner, a reader encountering an unfamiliar register, or anyone reading a text whose emotional valence is ambiguous—benefits from a system that makes the trajectory explicit rather than leaving it to be inferred.

The Prosodic Measurement Operator

This section formalizes prosody as a measurable physical structure by identifying the minimal set of signal events from which invariant quantities can be extracted. The key move is to replace uniform sampling with event-based sampling: instead of analyzing every point in the waveform, the system tracks peaks, which concentrate the signal's energetic and temporal structure.

Let $u(t)$ denote an acoustic waveform, a real-valued signal defined over a time interval $[0, T]$. A prosodic analysis of $u(t)$ extracts from it a finite-dimensional vector of physically interpretable invariants. The central object is the *prosodic measurement operator*

$$\mathcal{M} : u(t) \mapsto \mathcal{M}(u) \in \mathbb{R}^n, \tag{8}$$

which maps a waveform to a coordinate in prosodic parameter space. This is not an embedding in the machine-learning sense: the components of $\mathcal{M}(u)$ are not learned abstractions but measured physical quantities, computable from the peak structure of the waveform.

For a concrete and sufficient instantiation, let $\{t_k\}_{k=1}^{N}$ denote the sequence of peak times in $u(t)$ and $\{a_k\}_{k=1}^{N}$ the corresponding peak amplitudes. Define the inter-peak intervals $\Delta t_k = t_k - t_{k-1}$, the period jitter values $j_p(k) = |\Delta t_k - \overline{\Delta t}|/\overline{\Delta t}$, and the amplitude jitter values $j_a(k) = |a_k - \bar{a}|/\bar{a}$, where overbars denote sample means. The measurement operator then returns the eight-dimensional vector

$$\mathcal{M}(u) = \Big(\overline{j_p},\ \sigma_{j_p},\ \overline{j_a},\ \sigma_{j_a},\ h,\ s,\ \rho,\ E\Big) \in \mathbb{R}^8, \tag{9}$$

where $\overline{j_p}$ and σ_{j_p} are the mean and standard deviation of period jitter, $\overline{j_a}$ and σ_{j_a} are the mean and standard deviation of amplitude jitter, h measures harmonic coherence (the degree of periodic regularity in the voiced signal), $s = (1 + \overline{j_p} + \overline{j_a})^{-1}$ is a salience index that varies inversely with total jitter, $\rho = N/T$ is peak density in events per second, and $E = N^{-1} \sum_k a_k^2$ is mean squared amplitude.

Several features of this definition deserve emphasis. The vector is low-dimensional relative to the signal itself—eight scalars from a waveform of potentially millions of samples—but each dimension is physically interpretable and stable under small perturbations of the signal. It is not a compressed representation in the information-theoretic sense: it discards information, but the discarded information is precisely the within-utterance variation that prosody averages over. What remains are the *invariants* of prosodic structure: the statistical regularities that persist across different realizations of the same utterance.

The choice of eight dimensions is a concrete instance of a general principle. Any finite collection of measurable prosodic invariants defines a valid measurement operator; the specific vector (9) is used throughout this essay as a reference implementation, not as a claim that exactly these eight dimensions are necessary or complete.

Modal Storage: The MEM|8 Lattice Coordinate

This section replaces symbolic representation with geometric representation. Instead of storing linguistic identity as discrete labels, the system stores positions in a structured measurement space where similarity is a metric property rather than a categorical one.

The continuous prosodic vector $\mathcal{M}(u) \in \mathbb{R}^8$ can be quantized into a discrete modal coordinate through a fixed-point quantization operator

$$Q : \mathbb{R}^n \to \mathbb{Z}^n_{Q8.8}, \qquad Z_\alpha = Q(\mathcal{M}(u)), \tag{10}$$

where $\mathbb{Z}^n_{Q8.8}$ denotes the lattice of n-dimensional vectors with components in an 8.8 fixed-point format (8 bits integer part, 8 bits fractional part). The resulting vector Z_α is a *modal coordinate*: a discrete address in a resonance lattice that encodes the prosodic structure of the original waveform without storing semantic content.

This distinction is important. A modal coordinate is not a meaning; it is a position in a structured measurement space. Identity and similarity emerge from proximity in this space—from the inner product $\langle Z_\alpha, Z_\beta \rangle = \sum_i Z_\alpha[i] \cdot Z_\beta[i]$—rather than from symbolic labeling. Two utterances are similar when their modal coordinates are close, and their prosodic similarity is a measurable geometric fact about the lattice, not a judgment about linguistic content.

The MEM|8 system uses this coordinate as a probe: incoming audio is mapped to a modal vector, and the stored lattice is queried for nearby configurations. Retrieval is resonance rather than lookup, and similarity is geometric rather than symbolic. The full chain from audio to stored modal coordinate is

$$u(t) \xrightarrow{\mathcal{M}} \mathcal{M}(u) \xrightarrow{Q} Z_\alpha \in \mathbb{Z}^8_{Q8.8}. \tag{11}$$

Hyperbionic Typography as a Projection Operator

This section defines the visual projection of prosodic structure. The goal is not to visualize sound in an illustrative sense but to construct a mapping in which typography becomes a coordinate system for the same invariant quantities measured acoustically.

The third element of the framework is the visual projection. Let T_i be a text token with glyph g_i. We associate to it a prosodic parameter vector

$$p_i = (e_i, f_i, d_i, j_i, r_i, \delta_i, \phi_i, \eta_i) \in \mathbb{R}^m, \tag{12}$$

whose components correspond to energy, pitch, duration, jitter, reverberation, delay, phase, and affective intensity respectively. The *Hyperbionic rendering operator* is

$$\mathcal{H}(T_i, p_i) = R(g_i, p_i), \tag{13}$$

where R maps the glyph g_i and parameter vector p_i to a visual configuration. The visual degrees of freedom available to R include font size and weight (encoding energy), vertical baseline displacement (encoding pitch), inter-character and inter-word spacing (encoding duration), micro-rotation or distortion (encoding jitter), and opacity or layering (encoding salience). The result is that typography becomes a projection operator on prosodic space: the glyph is a carrier, and its visual properties are the signal.

The mapping from parameter to visual property is not arbitrary. It is constrained by two requirements: *monotonicity* (larger values of a parameter should produce consistently more or less of the corresponding visual property, not a non-monotone scrambling) and *legibility* (the mapping must preserve the readability of the underlying glyph across the full range of parameter values). These constraints define the admissible region of R: the set of parameter-to-visual mappings that produce coherent typography rather than visual noise. A minimal admissible mapping for the core parameters is given in Table 1.

Parameter	**Visual property**	**Direction**
Energy e_i	Font size / weight	Increasing
Pitch f_i	Baseline displacement	Upward
Duration d_i	Letter spacing	Wider
Jitter j_i	Micro-rotation	Increasing magnitude
Salience s_i	Opacity	Increasing

Table 1: Core prosodic parameter to visual property mappings under the admissibility constraints.

Equivalence of Representations

The preceding sections introduced three transformations of the same signal: measurement, quantization, and rendering. The question now is whether these transformations preserve a common structure, or whether each introduces incompatible distortions. The answer is that there exists a shared invariant, and each representation is a coordinate chart on that invariant. The three representations—acoustic measurement, modal lattice coordinate, and Hyperbionic rendering—are related by this structure. Define projection operators

$$\Pi_{\text{audio}}, \quad \Pi_{\text{mem}}, \quad \Pi_{\text{text}}, \tag{14}$$

which extract the shared prosodic invariants from an audio waveform, a MEM|8 modal vector, and a Hyperbionic rendering respectively. We say that three representations are *prosodically equivalent* when

$$\Pi_{\text{audio}}(u) = \Pi_{\text{mem}}(Z_\alpha) = \Pi_{\text{text}}(R(g, p)). \tag{15}$$

$$\Pi_{\text{audio}} = \Pi_{\text{mem}} = \Pi_{\text{text}}$$

This identity is not descriptive but prescriptive: it defines a hard constraint on system design. Any operator that violates invariant preservation is inadmissible. If R collapses distinctions that $\mathcal{M}$ preserves, or if Q introduces distinctions not present in the measured signal, the system fails at the level of representation.

To make the invariant structure precise, we introduce an explicit invariant object. Define

$$\mathcal{I}(u) := \Pi_{\text{audio}}(u), \tag{16}$$

and express the other projections as factorizations through the same invariant:

$$\Pi_{\text{mem}} = \mathcal{I} \circ Q^{-1}, \qquad \Pi_{\text{text}} = \mathcal{I} \circ R^{-1}. \tag{17}$$

The central identity (15) then becomes $\mathcal{I}(u) = \mathcal{I}(Z_\alpha) = \mathcal{I}(R(g,p))$: a single invariant object with three coordinate charts. This upgrades the framework from a family of commuting operators to a true invariant with multiple sections.

Proposition 1 (Invariant Preservation under Lossy Projection)**.** *The operators $\mathcal{M}$, Q, and R are not injective; however, they preserve the invariant $\mathcal{I}$. That is,*

$$x \neq y \;\not\Rightarrow\; \mathcal{I}(x) \neq \mathcal{I}(y), \qquad \textit{but} \qquad \mathcal{I}(x) = \mathcal{I}(y) \;\Rightarrow\; \textit{indistinguishable under all admissible projectio} \tag{18}$$

The system does not preserve waveforms; it preserves equivalence classes.

This equivalence is not the claim that audio, a lattice vector, and rendered typography are the same object. They are manifestly different objects in different media. The claim is that they are different parameterized projections of the same underlying invariant structure—that the prosodic content encoded in each is preserved under the chain of operators $\mathcal{M}$, Q, and R, modulo the information that each representation deliberately discards.

The three representations differ only in their output medium:

$$\begin{aligned} \mathcal{M} &: \text{sound} \to \mathbb{R}^8, \\ Q &: \mathbb{R}^8 \to \mathbb{Z}^8_{Q8.8}, \\ \mathcal{H} &: \text{text} \times \mathbb{R}^m \to \text{visual field.} \end{aligned}$$

Marine prosody measures invariants acoustically; MEM|8 stores them as modal lattice coordinates; Hyperbionic Reading renders them visually. The prosodic structure is conserved across transformations of medium.

This equivalence has a direct consequence for the ontological status of typographic markup. Plain text is a projection onto the subspace of lexical content, discarding all prosodic dimensions. Parameterized text—text annotated with a prosodic parameter vector p_i for each token—is a projection onto a higher-dimensional subspace that preserves prosodic as well as lexical structure. The inclusion is strict:

$$\text{plain text} \subset \text{parameterized text} \subset \text{multimodal resonance field}. \tag{19}$$

Marked-up text is not decorated language. It is a higher-dimensional prosodic encoding.

Extension to Higher-Dimensional Features: Delay and Reverberation

The parameter vector (12) can be extended to include acoustic features that go beyond basic prosody. Two such extensions are particularly natural: temporal delay and spatial reverberation. Both admit precise typographic operators, and both illustrate the general principle that acoustic signal processing operations have direct visual analogues.

Delay as a Spatial Duplication Operator

A delayed acoustic signal is modeled as

$$u_{\text{delay}}(t) = u(t) + \lambda\, u(t - \tau), \tag{20}$$

where $\tau > 0$ is the delay time and $\lambda \in (0, 1)$ is the attenuation factor. The delayed copy arrives later, at reduced amplitude. The typographic analogue is a spatial displacement operator:

$$R_{\text{delay}}(g, p) = R(g, p) + \lambda\, R(g, p;\, \Delta x(\tau), \Delta y(\tau), \alpha(\lambda))\,, \tag{21}$$

where $\Delta x(\tau)$ and $\Delta y(\tau)$ are horizontal and vertical offsets that increase with delay time τ, and $\alpha(\lambda) \in [0, 1]$ is the opacity of the echo glyph, decreasing with attenuation λ. Temporal delay becomes spatial displacement: a sound heard twice, the second time later and quieter, is rendered as a glyph seen twice, the second time offset and faded.

The correspondence is exact in the following sense: the ratio of echo amplitude to primary amplitude is λ in both the acoustic and typographic representations, and the direction of the offset $(\Delta x, \Delta y)$ can encode the azimuthal angle of the delay source (front/back, left/right) for spatialized audio effects.

Reverberation as a Convolutional Halo

Reverberation is the persistence of acoustic energy through multiple reflections in a bounded space. It is modeled as the convolution of the source signal with an impulse response:

$$u_{\text{reverb}}(t) = (u * k)(t) = \int u(s)\, k(t-s)\, ds, \tag{22}$$

where $k(t)$ is the room impulse response encoding the geometry and absorption properties of the space. The typographic analogue is a visual convolution operator:

$$R_{\text{reverb}}(g, p) = R(g, p) * K_{\text{visual}}, \tag{23}$$

where K_{visual} is a two-dimensional kernel whose support encodes the spatial extent of reverberation. A short, tight K_{visual} produces a slight glow or shadow; a broad K_{visual} produces an extended halo, trailing echoes, or a blur that increases with distance from the glyph center. Reverberation becomes spatial diffusion: acoustic energy that spreads through a room becomes visual density that spreads through the typographic field.

These two extensions illustrate a general structural principle. Acoustic time-domain operations—shifting, scaling, convolving—have exact analogues in visual space-domain operations—displacing, fading, blurring. The parameter space of acoustic signal processing and the parameter space of typographic rendering are not merely analogous; they are formally isomorphic under the correspondence $t \leftrightarrow x$ (time maps to horizontal position), $\lambda \leftrightarrow \alpha$ (amplitude maps to opacity), and $k(t) \leftrightarrow K_{\text{visual}}$ (temporal impulse response maps to spatial convolution kernel).

Speech as Trajectory: The Temporal Extension

This section addresses the central limitation of static representations: a single prosodic vector cannot capture temporal structure. To resolve this, the framework is extended from points to paths, treating speech as a continuous trajectory through parameter space and replacing classification with geometric alignment.

The framework so far treats each utterance as producing a single prosodic vector $\mathcal{M}(u) \in \mathbb{R}^8$. For isolated vowels or short, stable phonemes, this is adequate. For connected speech—for words and sentences whose prosodic structure evolves over time—a single vector is insufficient. A spoken word is not a point in prosodic space but a continuous curve through it.

This observation motivates the temporal extension of the framework. Define the *instantaneous prosodic measurement* as the prosodic vector computed over a short sliding window:

$$\gamma(t) = \mathcal{M}(u\restriction_{[t-\Delta,t]}) \in \mathbb{R}^8, \tag{24}$$

where $u\restriction_{[t-\Delta,t]}$ denotes the restriction of the waveform to the window $[t-\Delta, t]$. As t varies, $\gamma(t)$ traces a continuous path through prosodic parameter space. After quantization at discrete time steps $t_1, \ldots, t_K$, this path becomes a finite trajectory in the modal lattice:

$$\Gamma = \{Z_\alpha(t_k)\}_{k=1}^{K} \subset \mathbb{Z}^8_{Q8.8}. \tag{25}$$

A spoken word is thus represented not as a single modal coordinate but as a finite sequence of coordinates—a path through the lattice that encodes the temporal evolution of its prosodic structure.

Word Basins and Trajectory Resonance

The trajectory representation leads naturally to a wave-native architecture for speech recognition. Define a *word basin* as a stored reference trajectory

$$\mathcal{W}_i = \{Z_i(t_k)\}_{k=1}^{K_i} \tag{26}$$

associated with the i-th lexical item. Recognition of an incoming trajectory Γ against the stored dictionary $\mathcal{D} = \{(\mathcal{W}_i, \text{word}_i)\}$ is performed by a coherence functional that is invariant under temporal stretching and compression. Using dynamic time warping, this is

$$\mathcal{C}_{\text{DTW}}(\Gamma, \mathcal{W}_i) = \max_{\pi} \frac{1}{|\pi|} \sum_{(k,\ell)\in\pi} \frac{\langle Z_\alpha(t_k),\, Z_i(t_\ell)\rangle}{\|Z_\alpha(t_k)\|_Q \cdot \|Z_i(t_\ell)\|_Q + \varepsilon}, \tag{27}$$

where π ranges over admissible alignment paths, $\varepsilon > 0$ guards against zero-norm packets, and $\|\cdot\|_Q$ denotes the ℓ^2 norm in Q8.8 fixed-point arithmetic before rescaling. The normalized form keeps $\mathcal{C}_{\text{DTW}} \in [-1, 1]$ independent of recording level.

To prevent energy dimensions from swamping jitter dimensions—which behave as high-frequency discriminators while energy and density behave as low-frequency stabilizers—the inner product is replaced throughout by a G-weighted form:

$$\langle Z, Z' \rangle_G = Z^\top G Z', \qquad G = \mathrm{diag}(w_1, \ldots, w_8), \tag{28}$$

with corresponding norm $\|Z\|_G = \sqrt{\langle Z, Z \rangle_G}$. The DTW coherence then becomes

$$\mathcal{C}_{\mathrm{DTW}}(\Gamma, \mathcal{W}_i) = \max_\pi \frac{1}{|\pi|} \sum_{(k,\ell)\in\pi} \frac{\langle Z_\alpha(t_k),\, Z_i(t_\ell) \rangle_G}{\|Z_\alpha(t_k)\|_G \cdot \|Z_i(t_\ell)\|_G + \varepsilon}. \tag{29}$$

The weights w_i encode perceptual sensitivity: jitter dimensions receive higher weight than energy or density, reflecting the auditory system's greater sensitivity to timing irregularity than to absolute loudness. The prosodic parameter space is therefore not $\mathbb{R}^8$ in the ordinary Euclidean sense but the metric space $V = (\mathbb{R}^8, G)$; all norms, angles, and curvatures in the remainder of the paper are taken with respect to G. Recognition occurs when the maximum coherence across stored basins exceeds a threshold:

$$\hat{i} = \arg\max_i \, \mathcal{C}_{\mathrm{DTW}}(\Gamma, \mathcal{W}_i), \qquad \text{if } \mathcal{C}_{\mathrm{DTW}}(\Gamma, \mathcal{W}_{\hat{i}}) > \theta. \tag{30}$$

This replaces the classification paradigm of conventional automatic speech recognition—in which a trained statistical model maps fixed-length feature vectors to categorical labels—with a resonance paradigm in which stored trajectories are compared to incoming trajectories by a physically interpretable geometric functional.

The architecture has two phases. In the *teaching phase*, aligned audio-text pairs are processed: each audio segment is mapped through $\mathcal{M}$ and Q to produce a trajectory Γ, phoneme or word boundaries are detected using a harmonicity gate ($h(t) < \varepsilon$ signals a boundary between voiced and unvoiced regions), and the resulting trajectory is stored as a word basin $\mathcal{W}_i$. No gradient descent, no parameter optimization: the teaching phase populates a dictionary of trajectories. In the *detection phase*, a sliding trajectory window is maintained, and when the signal energy falls below a silence threshold, the current window is compared against all stored basins and the word with maximal coherence is emitted.

Trajectory Equivalence Across Modalities

The trajectory formulation extends the prosodic equivalence of Section 5 into the temporal domain. A sequence of Hyperbionic text tokens $\{T_i\}$ with parameter vectors $\{p_i\}$ defines a discrete path in typographic parameter space:

$$\Gamma_{\text{text}} = \{p_i\}_{i=1}^N. \tag{31}$$

The equivalence (15) then extends to trajectories:

$$\Gamma_{\text{audio}} \sim \Gamma_{\text{mem}} \sim \Gamma_{\text{text}}, \tag{32}$$

where equivalence is defined by preservation of prosodic invariants under projection. Speech-to-text is the operation $\Gamma_{\text{audio}} \to \Gamma_{\text{text}}$; text-to-speech is its inverse. Both are instances of trajectory reconstruction across modalities.

From Salience Packets to Modal Trajectories

The measurement operator $\mathcal{M}$, as previously defined, presents prosody as a direct mapping from waveform to vector. In practice, this mapping factors through a more primitive layer: a stream of discrete acoustic events. These events form the true substrate of the system, from which both statistical summaries and trajectories are derived. Formalizing this intermediate layer clarifies why the vector is not the fundamental object of the system, and motivates the trajectory representation as a natural consequence of event-based sampling rather than an additional design choice.

The Salience Packet as Fundamental Unit

The Marine processor does not sample the waveform uniformly. It samples *events*: local maxima of the signal that exceed the clip threshold and satisfy the period validity gate. Each detected peak emits a *salience packet*

$$\mathcal{P}_k = \big(j_p(k),\ j_a(k),\ h(k),\ s(k),\ E(k),\ t_k\big), \tag{33}$$

where $j_p(k)$ is period jitter, $j_a(k)$ is amplitude jitter, $h(k)$ is harmonic alignment, $s(k)$ is the salience score, $E(k) = a_k^2$ is local peak energy, and t_k is the sample index of the peak. The full output of the processor on a waveform segment is the ordered packet stream

$$u(t) \ \longrightarrow\ \{\mathcal{P}_k\}_{k=1}^{N}. \tag{34}$$

The packet stream can equivalently be viewed as a discrete measure over event time:

$$\mu_u = \sum_{k=1}^{N} \delta_{t_k} \cdot \mathcal{P}_k, \tag{35}$$

where δ_{t_k} is a Dirac mass at peak time t_k and $\mathcal{P}_k$ is the associated packet value. Under this representation, the prosodic vector $\mathcal{M}(u) = \mathcal{A}(\mu_u)$ is a moment functional on μ_u, and the trajectory $\Gamma = \{Z_\alpha(t_k)\}$ is the pushforward of μ_u under the quantization map $Q \circ \phi$. Aggregation and trajectory construction are therefore not two separate operations but two different functionals on the same underlying measure.

This event-based representation has three properties that distinguish it from uniform sampling. It is *sparse*: packets are emitted only at peaks, so the stream has $N \ll T \cdot f_s$ elements for a waveform of duration T. It is *physically grounded*: every component of $\mathcal{P}_k$ is a measured invariant of the signal, not a learned abstraction. And it is *approximately rate-invariant*: because peaks are detected by local comparison rather than by absolute time index, two recordings of the same utterance at different speaking rates produce packet streams with similar jitter profiles but different lengths, which is exactly the structure that the DTW coherence functional in Section 7 is designed to exploit.

The prosodic vector $\mathcal{M}(u)$ defined in equation (9) is now revealed as an *aggregation* of the packet stream rather than a direct measurement:

$$\mathcal{M}(u) = \mathcal{A}\big(\{\mathcal{P}_k\}_{k=1}^{N}\big), \tag{36}$$

where $\mathcal{A}$ computes the component-wise statistics (means, standard deviations, density, energy mean) defined in (9). The two-stage chain is then

$$u(t) \xrightarrow{\text{peak detection}} \{\mathcal{P}_k\} \xrightarrow{\mathcal{A}} \mathcal{M}(u) \xrightarrow{Q} Z_\alpha \in \mathbb{Z}^8_{Q8.8}, \tag{37}$$

making explicit that the packet stream is the primary object and the prosodic vector is a secondary, aggregate summary.

Packet-to-Modal Projection

The aggregation route (36) collapses temporal information: a vector $\mathcal{M}(u)$ contains no record of *when* within the utterance each packet was emitted. For identity and emotion classification this may be acceptable, but for trajectory-based speech recognition it is not. The alternative is to project each packet individually into a modal coordinate:

$$Z_\alpha(t_k) = Q\big(\phi(\mathcal{P}_k)\big) \in \mathbb{Z}^8_{Q8.8}, \tag{38}$$

where $\phi : \mathcal{P}_k \mapsto \mathbb{R}^8$ selects and possibly augments the packet components. A natural choice includes the six packet fields plus two local-variation terms:

$$\phi(\mathcal{P}_k) = \big(j_p(k),\ j_a(k),\ h(k),\ s(k),\ \rho(k),\ E(k),\ \Delta j_p(k),\ \Delta j_a(k)\big), \tag{39}$$

where $\rho(k)$ is the instantaneous peak density estimated in a short window around t_k, and $\Delta j_p(k) = j_p(k) - j_p(k-1)$, $\Delta j_a(k) = j_a(k) - j_a(k-1)$ are first differences capturing local acceleration of jitter. The per-packet projection (38) produces a sequence of modal vectors indexed by peak time, from which the trajectory $\Gamma = \{Z_\alpha(t_k)\}_{k=1}^N$ is directly obtained. The three-level hierarchy is then

$$\begin{aligned} \text{Local (event physics):} \quad & \mathcal{P}_k, \\ \text{Global (statistical identity):} \quad & \mathcal{M}(u) = \mathcal{A}(\{\mathcal{P}_k\}), \\ \text{Temporal (trajectory meaning):} \quad & \Gamma = \{Z_\alpha(t_k)\}_{k=1}^N. \end{aligned} \tag{40}$$

All three representations derive from the same packet stream. They are not competing descriptions but projections of the packet stream onto different summary statistics.

The SalienceMarker Enumeration as Topological Signal

The Marine processor does not emit only packets. Its output type is the enumeration

$$\text{SalienceMarker} \in \{\text{Peak}(\mathcal{P}_k),\ \text{Fracture},\ \text{Noise},\ \text{Insufficient}\}, \tag{41}$$

where Fracture marks silence or a gap in the signal (inter-peak period exceeding the validity gate), Noise marks a region of high-amplitude aperiodic signal (energy above the clip threshold but no coherent peaks), and Insufficient marks a region where the processor has not yet warmed up. This enumeration introduces topological structure into the signal: rather than a continuous function, the processor produces a partition of the timeline into structured regions (voiced, voiced-unstable), boundaries (fractures between voiced regions), and noise fields.

The Fracture marker is particularly important for the trajectory architecture. A trajectory Γ is a sequence of modal coordinates at peak times; a Fracture between two peaks creates a gap in the sequence that is not filled by interpolation. Word basins $\mathcal{W}_i$ therefore naturally encode the silence structure of the corresponding utterance, and the DTW alignment path π in equation (27) must skip over Fracture gaps in both the query and the stored basin consistently. The Fracture marker therefore induces a canonical decomposition of any trajectory into voiced components separated by silence boundaries:

$$\Gamma = \bigsqcup_m \Gamma_m, \tag{42}$$

where each Γ_m is a connected voiced segment and $\sqcup$ denotes disjoint union. DTW alignment is restricted to pairs within the same component; TARTAN tiles inherit this segmentation, with boundary flags $b_{\ell,j}$ propagating the Fracture structure up the hierarchy. In the Hyperbionic rendering, Fracture events correspond to typographic white space: the absence of prosodic transformation between adjacent tokens is itself a prosodic signal. The system thus maintains a clean distinction between two kinds of absence: silence removes points from Γ entirely (a topological gap in the trajectory), while low salience down-weights existing points in $\mathcal{C}$ without removing them (a geometric thinning of the trajectory). Conflating these two would misclassify quiet expressive passages as silence; the Fracture marker prevents this by requiring energy to fall below the clip threshold, not merely for salience to be low.

A Real Trajectory Space and TARTAN Multiscale Tiling

This section establishes the real geometric structure of trajectory space and introduces a multiscale organization required for stability. Raw trajectories are sensitive to local perturbations; TARTAN constructs a hierarchy that preserves global structure while isolating local noise, allowing recognition to operate at the appropriate scale. Its role is not compression but stabilization.

The trajectory representation $\Gamma = \{Z_\alpha(t_k)\}$ is powerful but fragile in a specific way: a small perturbation in a single packet—a spurious peak, a momentary noise spike—can shift the trajectory locally and degrade DTW coherence. A robust architecture requires a multiscale organization that separates global word shape from local packet noise.

The Real Trajectory Space

Before introducing the multiscale structure, it is useful to state the trajectory space precisely. After rescaling the fixed-point vectors to real values, each modal coordinate is an element of $V = \mathbb{R}^8$, and the inner product is the ordinary real dot product

$$\langle Z, Z' \rangle = \sum_{i=1}^{8} Z_i Z'_i. \tag{43}$$

No imaginary components are required.

Proposition 2 (Geometric Phase Representation)**.** *Let $\Gamma \subset \mathbb{R}^8$ be a trajectory in modal space V. All phase-dependent interference effects are representable as geometric relations on Γ under the real inner product structure of V. No complex extension is required.*

Phase mismatch corresponds to trajectory divergence under alignment: two trajectories that would destructively interfere in a complex-exponential model appear as misaligned paths under the DTW coherence functional, yielding low or negative $\mathcal{C}$. Phase-like structure is represented geometrically by the direction of trajectory movement through modal space, not by imaginary coefficients. The space of finite trajectories of any length is $\mathcal{T} = \bigcup_{N \geq 1} V^N$, and the normalized coherence between two trajectories under an alignment path π is

$$\mathcal{C}(\Gamma, \Gamma') = \frac{1}{|\pi|} \sum_{(k,\ell) \in \pi} \frac{\langle Z_\alpha(t_k), Z'_\alpha(t_\ell) \rangle}{\|Z_\alpha(t_k)\| \cdot \|Z'_\alpha(t_\ell)\| + \varepsilon}, \tag{44}$$

where $\varepsilon > 0$ prevents division by zero for silent or near-zero packets. The coherence is in $[-1, 1]$, with $\mathcal{C} = 1$ indicating perfect alignment and $\mathcal{C} \leq 0$ indicating destructive interference: the two trajectories are moving in incompatible directions in modal space at the aligned time steps.

TARTAN: Trajectory-Aware Recursive Tiling with Annotated Noise

A raw trajectory $\Gamma = \{Z_\alpha(t_k)\}_{k=1}^N$ operates at the finest temporal scale—one modal vector per detected peak. For recognition, retrieval, and storage, it is advantageous to organize this fine-grained sequence into a hierarchy of coarser approximations. The TARTAN framework provides this organization.

TARTAN maps a raw trajectory to a sequence of tiled approximations at increasing coarseness levels:

$$\Gamma \longrightarrow \mathcal{T}_0(\Gamma),\ \mathcal{T}_1(\Gamma),\ \ldots,\ \mathcal{T}_L(\Gamma), \tag{45}$$

where $\mathcal{T}_0(\Gamma) = \Gamma$ is the original packet-level trajectory and each $\mathcal{T}_{\ell+1}$ is obtained by recursively tiling $\mathcal{T}_\ell$: partitioning it into non-overlapping segments and replacing each segment with a local summary tile

$$\tau_{\ell,j} = \big(\bar{Z}_{\ell,j},\ \Sigma_{\ell,j},\ \eta_{\ell,j},\ b_{\ell,j}\big), \tag{46}$$

where $\bar{Z}_{\ell,j}$ is the mean modal vector over the segment, $\Sigma_{\ell,j}$ is a scalar or diagonal measure of local variance, $\eta_{\ell,j}$ is an annotated noise estimate (derived from the Noise markers in the SalienceMarker stream), and $b_{\ell,j} \in \{0, 1\}$ is a boundary flag marking whether a Fracture occurred within the segment.

The boundary flag is the key innovation: by propagating Fracture information up the tiling hierarchy, TARTAN ensures that silence structure is preserved at every scale. A coarse tile spanning a silence boundary is annotated as such, so that alignment at the coarse level does not inadvertently match voiced content across a silence gap.

Multiscale recognition proceeds by computing a weighted coherence across levels:

$$\mathcal{C}_{\text{TARTAN}}(\Gamma, \Gamma') = \sum_{\ell=0}^{L} w_\ell \, \mathcal{C}\big(\mathcal{T}_\ell(\Gamma),\ \mathcal{T}_\ell(\Gamma')\big), \tag{47}$$

where the weights satisfy

$$\sum_{\ell=0}^{L} w_\ell = 1, \qquad w_0 \geq w_1 \geq \cdots \geq w_L > 0, \tag{48}$$

enforcing coarse-to-fine dominance. This normalization ensures that $\mathcal{C}_{\text{TARTAN}} \in [-1, 1]$ whenever each level coherence is normalized, and the monotone decrease prevents fine-level packet noise from destabilizing recognition. At coarse levels the system detects global word shape; at fine levels it verifies local prosodic microstructure. Recognition requires $\mathcal{C}_{\text{TARTAN}}(\Gamma, \mathcal{W}_i) > \theta$ for a stored word basin $\mathcal{W}_i$.

The Complete Equivalence

With all components in place, the full processing pipeline is

$$u(t) \xrightarrow{\text{Marine}} \{\mathcal{P}_k\} \xrightarrow{\phi, Q} \{Z_\alpha(t_k)\} \xrightarrow{\text{TARTAN}} \{\mathcal{T}_\ell(\Gamma)\}_{\ell=0}^{L}, \tag{49}$$

and the Hyperbionic visual trajectory $\Gamma_{\text{text}} = \{p_i\}$ is a rendering of the same packet-derived structure into typographic parameter space. The equivalence (32) therefore extends to include the TARTAN representation:

$$\Gamma_{\text{audio}} \sim \Gamma_{\text{mem}} \sim \Gamma_{\text{tartan}} \sim \Gamma_{\text{text}}, \tag{50}$$

where equivalence is preservation of prosodic invariants under admissible projection at each stage. The four components of the system have distinct roles that are now precisely delineated: Marine performs event extraction, MEM|8 provides modal storage of quantized packet coordinates, TARTAN organizes trajectories into multiscale tiles that are robust to local packet noise, and Hyperbionic Reading renders the same trajectory structure as a visual field. None of these roles overlaps; each is a necessary stage in the pipeline from acoustic signal to visual prosody.

Reconstruction and Cue-Based Retrieval

The bidirectionality of the framework raises a question about information recovery. Given a Hyperbionic rendering $R(g, p)$, can the original prosodic structure be recovered? The answer depends on which components of p are preserved under rendering and which are collapsed in the visual output.

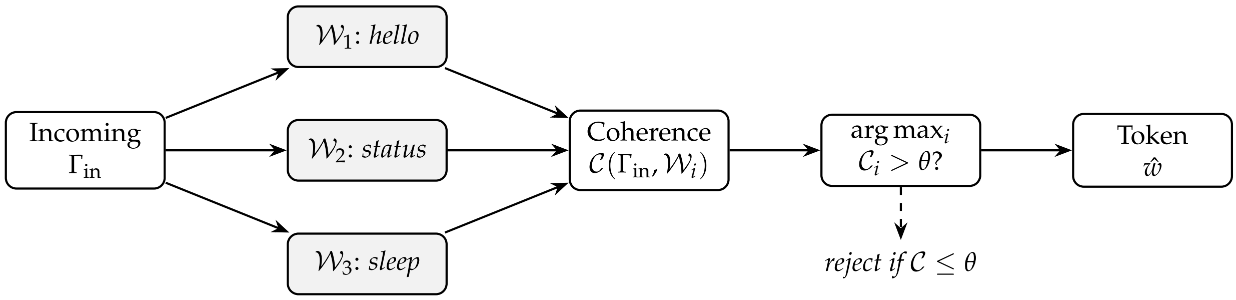

Figure 1: Trajectory resonance recognition. The incoming trajectory Γ_{in} is compared against all stored word basins by the DTW coherence functional (27). Recognition collapses onto the basin with maximal coherence exceeding threshold θ; trajectories with no basin above threshold are rejected. No classifier, no softmax: recognition is geometric collapse.

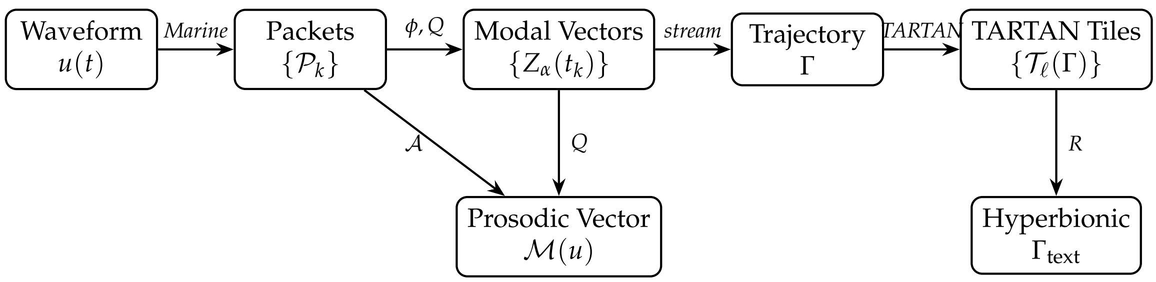

Figure 2: Full processing pipeline. The waveform $u(t)$ is converted by the Marine processor into a sparse packet stream $\{\mathcal{P}_k\}$. Per-packet projection ϕ followed by quantization Q yields modal vectors; their sequence is the trajectory Γ. TARTAN organizes Γ into a multiscale tile hierarchy. Aggregation $\mathcal{A}$ collapses the packet stream to the prosodic vector $\mathcal{M}(u)$ (statistical identity path). The Hyperbionic rendering operator R projects the tiled trajectory into the visual field.

For the core parameters in Table 1, the mapping is injective in principle: given a rendered glyph and knowledge of the rendering operator R, the parameter vector p can be extracted by inverting the visual-to-parameter correspondences. In practice, quantization and rendering resolution introduce information loss, but the loss is bounded by the same constraints that govern the admissibility of R: a rendering that is legible is one that preserves enough visual variation to make the parameter vector recoverable.

This recovery structure corresponds to what Tulving identified as *synergistic ecphory*: the process by which a partial retrieval cue, combined with stored engram information, produces a recollective state that neither the cue nor the engram alone determines [1]. Hyperbionic text functions as a structured cue set for prosodic reconstruction. The rendered glyph is the cue; the stored prosodic vector (or, in the MEM|8 case, the modal lattice coordinate) is the engram; and the reconstructed acoustic impression is their joint product. The full reconstruction chain is

$$R(g,p) \xrightarrow{R^{-1}} p \xrightarrow{Q^{-1}} \mathcal{M}(u) \xrightarrow{\text{synthesis}} \hat{u}(t), \tag{51}$$

where $\hat{u}(t)$ is a reconstructed waveform consistent with the recovered prosodic vector. This is not lossless reconstruction of the original waveform—the measurement operator $\mathcal{M}$ is many-to-one, and distinct waveforms with the same prosodic vector are indistinguishable at the level of (9)—but it is reconstruction of prosodic structure, which is precisely the structure that plain text discards and Hyperbionic rendering preserves.

Orthographic Invariance Under Visual Transformation

The preceding sections treat the glyph g_i as fixed while the prosodic parameter vector p_i varies. This section removes that assumption. A second, independent axis of transformation acts on the carrier itself, substituting one graphemic system for another while holding the underlying symbolic sequence, and therefore its meaning, fixed. Formalizing this axis is what allows $R(g_i, p_i)$ to generalize to $R(T_\theta(g_i), p_i)$: prosodic rendering applied to any admissible carrier, not only the Latin one.

The Carrier Transformation

Let X denote a symbolic sequence, a string of character identities independent of any particular glyph rendering, and let

$$T_\theta : X \longmapsto Y_\theta \tag{52}$$

be a carrier transformation indexed by θ: a substitution mapping each character identity in X onto a glyph drawn from an alternative graphemic system. The defining admissibility condition on T_θ is semantic invariance,

$$\mathrm{sem}(T_\theta X) = \mathrm{sem}(X), \tag{53}$$

which holds whenever T_θ is a consistent bijection on the alphabet: every instance of a given character maps to the same substitute glyph throughout X, so the sequence remains decodable in principle regardless of whether it is decodable in practice by a given reader. This is a stronger and more specific claim than the general admissibility condition of Section 16, which governs legibility of the prosodic field p; (53) governs identity of the underlying sequence under substitution of the carrier itself.

Composing T_θ with the Hyperbionic rendering operator gives the general form

$$R\big(T_\theta(g_i),\, p_i\big), \tag{54}$$

of which every rendering discussed so far, $R(g_i, p_i)$ with g_i a Latin glyph, is the special case $\theta = \mathrm{id}$. Nothing in the definitions of $\mathcal{M}$, Q, or R depends on the carrier being Latin; the prosodic parameter vector p_i is carrier-agnostic by construction, since it is extracted from the acoustic signal rather than from the glyph. The carrier and the field it carries are therefore independent degrees of freedom, and T_θ and $R(\cdot, p)$ commute: prosodic rendering can be applied to any admissible carrier, and a carrier can be substituted underneath an already-rendered prosodic field, without either operation constraining the other.

Symbolic Statistics Versus Perceptual Statistics

Because T_θ is required to be a consistent bijection, it preserves every statistic of the underlying symbolic process. If $H(X)$ denotes the entropy of the character sequence under whatever language model generates it,

$$H(X) = H(T_\theta X) \tag{55}$$

for any admissible θ: relabeling the alphabet does not change how predictable the sequence is at the symbolic level. But the decoding cost a reader actually incurs, $D_{\mathcal{R}}(X)$, the effort of the recognition process described in Section 15, equation (73), is not carrier-invariant:

$$D_{\mathcal{R}}(X) \neq D_{\mathcal{R}}(T_\theta X) \tag{56}$$

in general. Symbolic statistics are a property of the sequence; perceptual statistics are a property of the reader's relationship to a particular carrier rendering that sequence. A substitution alphabet can be information-theoretically transparent, carrying exactly the same predictive structure as the source language, while being perceptually opaque, imposing a large $D_{\mathcal{R}}$ because the reader has no learned mapping from the new glyphs to the symbols they encode. This is the precise sense in which T_θ is a distinct object from R: R varies perceptual cost by adding structured evidence to a fixed carrier; T_θ varies perceptual cost by changing which carrier bears the sequence at all, while H stays fixed throughout.

A Published Instance of the Transformation

This is not merely a proposed design space; a working family of admissible T_θ already exists as the `standardgalactic/fonts` repository, and a single essay has been rendered under several of them as a direct, checkable demonstration of (53). The repository defines carrier systems including Standard Galactic (`Sga-Regular`), a cursive variant (`CursiveGalactic-Regular`), Logico Philosophicus (`Logico_philosophicus-Regular`), Clypto (`Clypto-Regular`), a digit face in which magnitude is rendered as size (Dactyl, discussed in Section 27), and further variants (Shapeform, Cheiro, Systada, NovaMonoStandardGalactic, Amiri, a conventional Latin control, and a Lingojam-style cipher), each a distinct bijective substitution on the Latin alphabet together with a rendering font. A companion live tool exposes T_θ directly: a two-pane interface takes arbitrary typed text in one pane and renders it under a selected carrier in the other, letting a reader apply any T_θ to any X on demand rather than only to pre-generated examples.

The clearest demonstration, however, is a single essay, "The Vocabulary of Acceleration," published as parallel documents at URLs of the form `rhetoric/variants/vocabulary-of-acceleration-{Variant}`, one per carrier. The same symbolic sequence X, title, abstract, section structure, argument, appears at `-Sga` rendered in Standard Galactic, at `-Logico` rendered in Logico Philosophicus, at `-Clypto` rendered in Clypto, and under further variants, each satisfying $\mathrm{sem}(T_\theta X) = \mathrm{sem}(X)$ by construction, since all are generated from one source document, while differing sharply in $D_{\mathcal{R}}$. Standard Galactic imposes a moderate decoding cost: its glyphs are unfamiliar but each has a single, learnable Latin counterpart, so a reader with the key can decode letter by letter. Logico Philosophicus imposes a substantially higher cost: its glyph inventory is drawn from mathematical and logical operators ($\leq$, $\div$, $+$, %, $\perp$) with no inherent visual kinship to Latin letterforms, so decoding depends entirely on a memorized arbitrary mapping rather than any transferable visual intuition. Clypto imposes a comparatively lower cost despite equally unfamiliar graphemes, for the reason given in Section 15: its page-level statistics, ascender and descender rhythm, stroke continuity, baseline behavior, carry the typographic signature of ordinary handwriting, so a reader registers structural familiarity and partial word-shape cues even while unable to name a single letter. Comparing the same text across these renderings therefore gives a real, ranked instance of (56), holding $H(X)$ fixed by construction and varying only θ.

The same sequence, five carriers: identical symbolic statistics, five different decoding costs.

Every variant currently instantiated in this way sets $p = \mathbf{0}$: the carrier is substituted, but no prosodic field has yet been layered onto the substituted glyphs. The natural extension suggested by (54) is to apply Hyperbionic rendering on top of a chosen carrier, $R(T_\theta(g_i), p_i)$ with $\theta \neq \mathrm{id}$, producing, for instance, a Standard Galactic or Clypto rendering in which prosodic emphasis, timing, and jitter are additionally encoded in size, baseline, and spacing exactly as they are for the Latin carrier in the rest of this essay. Because T_θ and $R(\cdot, p)$ are independent operators acting on disjoint degrees of freedom, carrier and field, nothing in the framework developed so far prevents this composition; the existing carrier family supplies the substrate on which it remains to be built.

A Literal Implementation: Rendering-Only Ciphers

The strongest possible evidence for (53), that T_θ can leave $\mathrm{sem}(X)$ exactly fixed, is a working implementation in which the underlying character data is provably untouched and only the rendering function differs. Such an implementation exists as an interactive cipher puzzle built on the carrier fonts already discussed. Its source is instructive in a way a rendered specimen cannot be, because it exposes T_θ as a line of application code rather than a design claim about a font.

The puzzle stores the source phrase as an ordinary JavaScript string and assigns it to the DOM with a single line, `puzzleTextEl.textContent = phrase`, performing no character substitution, remapping, or encoding of any kind. The entire visual transformation is produced by a CSS rule attached to the containing element, `font-family: 'Logico Philosophicus', monospace`, and a companion rule for Standard Galactic. Selecting a different carrier is implemented as toggling a class on the document body; the underlying `textContent` of every element is never rewritten. This is T_θ realized with the identity map on the symbolic layer and all of the transformation pushed into the observation function:

$$X \xrightarrow{G_T} g \xrightarrow{R_p} V, \qquad V = R_p\big(G_T(X)\big), \tag{57}$$

where G_T names explicitly what (54) left implicit in the notation $T_\theta(g_i)$: a step that fixes which carrier realizes the character identities of X as glyphs g, prior to and independent of the prosodic rendering step R_p that was this essay's original subject. In the puzzle's implementation, G_T is nothing more than a font-family declaration, which is precisely why it is such clean evidence: there is no possible sense in which the character sequence has been altered, since the browser's own text layer, on which search, copy, screen-reader access, and the DOM's own string operations all still operate, contains the unmodified Latin string throughout. $\text{sem}(T_\theta X) = \text{sem}(X)$ is not an assumption to be verified here; it is a consequence of T_θ never having touched X at all.

The puzzle mechanic built on top of this rendering gives a direct way to operationalize the decoding cost $D_{\mathcal{R}}$ used throughout this section. Let $\tau_R(T)$ be the time a reader R requires to recover X from a specimen rendered under carrier T, and define a decoding cost relative to a fluent baseline,

$$D_R(T) = \frac{\tau_R(T)}{\tau_R(\text{Courier})}, \tag{58}$$

normalizing against the same reader's time on the ordinary Latin rendering rather than against an absolute clock, so that the measure reflects carrier difficulty rather than reading speed in general. Repeated puzzles let D_R be tracked as a function of accumulated exposure n, $D_R(T, n)$, which should decrease as a reader's inverse perceptual map from V_T back to X improves, giving the informal fluency progression described throughout this essay, chart lookup, then serial per-glyph decoding, then whole-word recognition, a directly measurable trajectory rather than only an introspective report.

The puzzle's Hint control is worth isolating as a model of how that trajectory actually proceeds. It does not reveal additional information about X; the underlying mapping the reader is reconstructing, call it $\widehat{M}$, is already fully determined by what the reader has entered. Hint instead performs selective rejection of inconsistent hypotheses,

$$\widehat{M}(a) \neq a \implies \widehat{M}(a) \leftarrow \varnothing, \tag{59}$$

clearing exactly the guesses that are wrong while leaving correct guesses in place. Recognition under an unfamiliar carrier therefore proceeds by repeated proposal, rejection of hypotheses inconsistent with the constraints already accumulated, retention of the rest, and further proposal, the same propose-reject-retain structure that governs the recognition equation of Section 15, $P(g_i \mid V_i, G_w, N, C)$, where visible evidence, word geometry, n-gram statistics, and sentence context jointly narrow a hypothesis space rather than each independently determining an answer. The puzzle differs from ordinary reading only in making that narrowing an explicit, externally visible action instead of an implicit perceptual one.

Three Separable Evaluation Quantities

Comparing carriers by decoding cost alone, as in the ranking above, conflates three quantities that a family of admissible T_θ makes possible to separate. The first is preserved information,

$$I(X;Y_i), \qquad Y_i = T_{\theta_i}(X), \tag{60}$$

which for any bijective substitution carrier is essentially maximal by construction, this is exactly the content of (55), and is not where the carriers differ. The second is reader-relative decoding cost,

$$C_{\mathcal{R}}(Y_i), \tag{61}$$

the effort a given reader incurs recovering X from Y_i, identical in kind to $D_{\mathcal{R}}$ above and the quantity the Sga/Logico/Clypto ranking actually measured, and operationalizable directly as the relative timing measure $D_R(T)$ of (58). The third is robustness under a family of further perturbations Θ, rotation, shear, blur, scale reduction, partial occlusion,

$$\mathcal{R}(Y_i, \Theta) = \inf_{\vartheta \in \Theta} P\big(\text{recognition survives } \vartheta(Y_i)\big), \tag{62}$$

which asks not how costly Y_i is to decode under ideal presentation but how much of that decodability degrades under further stress. These three need not co-vary: a carrier can preserve information maximally while imposing high decoding cost (Logico Philosophicus), and two carriers with comparable decoding cost can differ sharply in robustness if one encodes identity in features that survive rotation and blur, strong baseline, redundant height and width cues, and the other encodes identity in features that do not, fine internal stroke detail near a collision boundary. A carrier family is therefore not fully characterized by a single legibility ranking; it occupies a three-dimensional evaluation space, and the published variants, which already vary enormously in how they distribute visual redundancy, give a real corpus for populating it rather than a purely notional one.

Glyph Identity, Perceptual Margin, and the Collision Problem

Section 12 treats a carrier transformation T_θ as admissible whenever it is a consistent bijection on the alphabet. That condition is necessary but not sufficient for a carrier to be usable: a bijection can map two distinct source characters to glyphs so visually similar that a reader confuses them, which is a failure of the rendering rather than of the mapping.

This section makes precise what a single glyph's identity consists of, and works through a documented case, in which a design constraint intended to unify a script's visual grammar collapsed three characters together and forced the invention of a new distinguishing feature.

The Glyph as an Equivalence Class

A glyph g is not usefully identified with one fixed drawing. Handwriting varies a character's proportions from instance to instance; a typeface family renders it in weights, widths, and styles that share nothing pixel for pixel; and a single writer's own hand drifts over years of use. What is fixed is not the drawing but a set of drawings a reader accepts as the same character. Define the equivalence class of admissible realizations of g as

$$[g] = \{g' : g' \sim g\}, \tag{63}$$

where $g' \sim g$ holds exactly when a competent reader recognizes g' as the same character as g despite their differing as drawings. Typeface and handwriting variation explores the interior of $[g]$: bolding, slanting, condensing, and ordinary handwriting drift all produce realizations that remain inside the class. The design problem that actually threatens legibility sits at the boundary of $[g]$, the region where a member of $[g]$ becomes close, in whatever visual metric d governs perception, to a member of a different glyph's class $[h]$:

$$d(g', h') < \varepsilon \tag{64}$$

for some $g' \in [g]$, $h' \in [h]$. Crossing that boundary is a collision: two characters that are supposed to be distinguishable become, under some admissible deformation of each, indistinguishable.

This motivates a quantity that a mature script can be evaluated by and a young one cannot yet report: the perceptual margin of a glyph,

$$\Delta(g_i) = \min_{j \neq i} d(g_i, g_j), \tag{65}$$

the distance from g_i to its nearest neighbor in the alphabet. A newly designed script benefits from maximizing this margin before pursuing any other typographic goal, economy of stroke, aesthetic coherence, resemblance to an existing writing system, because every other refinement subsequently has to preserve $\Delta(g_i) > 0$ for all i rather than merely produce individually attractive characters. An alphabet chart, which shows each glyph once in isolation, cannot expose a small margin; only continuous text, where realizations drawn from across each $[g_i]$ actually occur adjacent to one another, can.

A Worked Collision: The Connected-Stroke Constraint

A documented case shows this mechanism concretely. A cursive variant of an existing block-letter script was built under an explicit design rule: no isolated dots, no detached strokes, every glyph a single continuous gesture. Formally, admissible glyphs g under this cursive system satisfy

$$\min C(g) \quad \text{subject to} \quad L(g) = 1, \qquad D(g) = 0, \qquad d_P(g_i, g_j) > \varepsilon, \tag{66}$$

where C is a gesture-complexity cost, $L(g) = 1$ requires the glyph to be drawable as one continuous path, $D(g) = 0$ forbids detached components, and d_P is the perceptual-distance margin of (65) applied under this constraint set. The constraint $D(g) = 0$ is exactly what makes the problem nontrivial: whatever information the block-letter ancestor script had encoded through a detached mark, an isolated dot, a separate bar, is no longer available to the cursive descendant, because that entire category of feature has been ruled inadmissible.

Three characters in the block ancestor were distinguished partly through such detached or rigid features. Under the connected-stroke projection, all three converged toward the same continuous-gesture neighborhood:

$$g_O,\ g_T,\ g_N \xrightarrow{\text{connect, remove detached marks}} \{\text{near-identical continuous gestures}\}.$$

The resolution was not to restore the forbidden feature, which would have violated $D(g) = 0$ and broken the stylistic coherence the constraint was designed to produce, but to introduce a new deformation native to continuous motion: a hook terminal, absent from the block ancestor, added specifically to g_N to reopen its margin from g_O and g_T. The hook is not decorative. It is the feature that satisfies $d_P(g_N, g_O) > \varepsilon$ and $d_P(g_N, g_T) > \varepsilon$ once every feature the constraint set had ruled out was no longer available to do that work.

A collision under a design constraint does not call for restoring the forbidden feature. It calls for discovering which feature the constraint still permits.

The general lesson generalizes past this one script. Whenever a carrier transformation T_θ imposes a global stylistic constraint, uniform stroke width, a fixed vertical band, connectedness, some subset of the source alphabet's distinguishing features becomes unavailable to every glyph simultaneously, and collisions among glyphs that had relied on exactly that feature are not a design failure so much as a diagnostic: they identify which features of the source script were carrying disambiguating information that the constraint has removed, and they force the constrained script to locate a replacement feature within whatever degrees of freedom the constraint still leaves open.

Readable Descendants and the Tactile Continuum

Every carrier discussed so far exists as one fixed design. This section treats the carrier's own difficulty as a tunable parameter rather than a fixed property, first by deriving an explicitly readable descendant from a deliberately difficult canonical form without altering the canonical form itself, and then by pushing the same reduction further, past ordinary readability and into a tactile encoding that shares no visual channel with the source at all.

Readability as a Branch, Not a Correction

A carrier designed to be difficult to read, deliberately unfamiliar glyphs, minimal redundancy, need not be modified in place to become easier. Its difficulty and its identity are not the same property, and a family of readable descendants can be derived while the canonical difficult form is left untouched:

$$G_{\text{canonical}} \xrightarrow{R_\lambda} G_{\text{readable}}, \tag{67}$$

where λ indexes the amount of perceptual assistance added. At $\lambda = 0$, R_0 is the identity and the canonical, cipher-like form is unchanged. Increasing λ progressively enlarges case contrast, differentiates height classes, widens inter-glyph spacing, separates characters near their collision boundary in the sense of (64), deepens descenders, and strengthens whatever disambiguating features, such as the hook of Section 13, the script has already discovered. Because R_λ acts on the same underlying glyph identities as T_θ acts on the same underlying symbolic sequence, an admissibility condition of the same shape as (53) applies: R_λ is legitimate only where it preserves the glyph identities of $G_{\text{canonical}}$, adding redundancy rather than introducing a different alphabet under the same name.

Treating readability this way turns a single fixed script into a controllable experimental family rather than a binary choice between one hard design and one easy redesign. Generating several intermediate $G_{\text{readable}}(\lambda)$ and measuring decoding cost $C_{\mathcal{R}}$ against λ can locate where legibility improves gradually and where it jumps, a single readability parameter, such as case contrast or height-class differentiation, may contribute little on its own while combining with a second parameter to produce a disproportionate improvement, exactly the kind of interaction a single before/after comparison cannot expose.

The Tactile Limit

Pushed far enough in the opposite direction from R_λ, the reduction that produced a legible cursive descendant from a block-letter ancestor can be iterated again, and again, until the representation is no longer visual at all. Each step removes further degrees of freedom while attempting to preserve the symbol distinction it started with:

$$G_{\text{standard}} \xrightarrow{\pi_1} G_{\text{cursive}} \xrightarrow{\pi_2} G_{\text{tactile}} \xrightarrow{\pi_3} B, \tag{68}$$

where each π_i satisfies the same non-collapsing requirement as every admissible projection in this essay,

$$g_i \neq g_j \quad \Longrightarrow \quad \pi(g_i) \neq \pi(g_j),$$

and B denotes a Braille-like tactile encoding. This is not a claim that such a system would or should outperform Braille as a mature tactile code; it is a claim about what the intermediate stage G_{tactile} would have to preserve to remain a genealogical descendant of G_{standard} rather than an unrelated replacement for it. A curve becomes two or three salient points; a terminal becomes an offset dot; relative height becomes row occupancy; left/right orientation becomes column occupancy. What survives this entire chain is not any particular stroke, since strokes are exactly what each π_i discards, but a small relational structure,

$$g_i \;\mapsto\; (V_i, E_i, \rho_i), \tag{69}$$

where V_i are the glyph's salient features, E_i their relationships, and ρ_i their coarse spatial placement. G_{standard} renders this graph richly, with stroke geometry, height, and scale all available as channels; G_{cursive} compresses it under the connected-stroke constraint of Section 13; a tactile descendant would render only the graph's nodes and relations, discarding the stroke entirely. The invariant that makes g_i recognizably g_i across the whole chain was therefore never the drawing. It was always (V_i, E_i, ρ_i), and every carrier in this essay, Latin, Standard Galactic, Cursive Galactic, Logico Philosophicus, Clypto, is one more coordinate chart rendering that same relational object, in exactly the sense that Section 12 makes precise for symbolic sequences and Section 6 makes precise for prosodic trajectories.

Across every carrier in this chain, the drawing changes completely. The relational graph it renders does not.

Clypto: The Destructive Dual of Hyperbionic Rendering

Section 12 treats carrier substitution T_θ as identity-preserving: every glyph survives, only its shape changes. This section treats a transformation that does not preserve every glyph: the controlled removal of visual evidence from a fixed carrier. Clipping is therefore not a sixth carrier alongside Standard Galactic, Logico, and the rest, but an operator that can be applied to any of them, including the Latin one, and the repository's own degradation tooling, sequenced font variants, an OCR-based recognition harness, and a document generator that renders progressively degrading text, already implements exactly this operator empirically.

The preceding sections develop R as an operator that adds structured visual evidence to a glyph. This section introduces a complementary operator that removes visual evidence instead, and shows that the two are not opposed techniques but coordinates of the same admissibility framework: one approaches the legibility boundary $C_{\max}$ from within, the other from without.

Everything so far has treated the rendering operator R as strictly additive: it takes a plain glyph g_i and a prosodic parameter vector p_i and returns a visually enriched configuration. But the admissibility framework developed in Section 16 already implies the existence of a dual operation. If R can add structured evidence up to a legibility ceiling $C_{\max}$, an operator that subtracts evidence down toward a legibility floor is equally well-defined, and equally informative about where meaning actually lives in a glyph.

The Clipping Operator

Let g be a glyph and define the *clipping operator*

$$C_\lambda(g), \qquad 0 \le \lambda \le 1, \tag{70}$$

which returns g with a fraction λ of its visual evidence removed—strokes truncated, terminals erased, connecting segments deleted—while leaving the underlying character identity, spacing, and linguistic context untouched. At $\lambda = 0$ the glyph is intact; as λ increases, progressively less visual evidence survives. Unlike R, which is parameterized by a measured prosodic vector, C_λ is parameterized by a single scalar erosion depth, which makes it an unusually clean experimental instrument: one dial, continuously tunable, that degrades exactly one thing.

Readability does not fall linearly in λ:

$$\mathcal{R}(\lambda) \not\approx 1 - \lambda. \tag{71}$$

Ten or twenty percent of a glyph can often be removed with no perceptible effect, because the removed strokes are visually redundant, before clipping crosses a feature that recognition actually depends on and legibility collapses abruptly. Each glyph therefore has its own *critical clipping threshold*

$$\lambda_i^* = \sup\{\lambda : \text{glyph } i \text{ remains reliably identifiable}\}, \tag{72}$$

and words inherit thresholds of their own that are not simply the minimum over their letters, because a clipped character that is locally ambiguous can still be resolved by its neighbors.

Recognition as Evidence Accumulation Across Sources

A clipped glyph is rarely read in isolation. Recognition draws on visible fragments (bottom-up evidence), the surviving silhouette of the whole word (orthographic evidence), the statistics of which letter sequences are plausible (an n-gram prior), and the surrounding sentence (a semantic prior):

$$P(g_i \mid V_i, G_w, N, C), \tag{73}$$

where V_i is the remaining glyph evidence after clipping, G_w is the global shape of the containing word, N is n-gram plausibility, and C is broader linguistic context. This makes the critical threshold a property not of the glyph alone but of the whole recognition context in which it sits:

$$\lambda^*(g \mid R,\, w,\, c,\, T), \tag{74}$$

parameterized by the reader R, the containing word w, the linguistic context c, and the writing system T. The same physical erosion can be recoverable in one context and unrecoverable in another, because what fails is not the glyph but the joint evidence available for reconstructing it.

Combining the Two Operators

Because R adds structured evidence and C_λ removes raw evidence, the two compose into a single two-parameter family

$$Y_{\alpha,\beta} = C_\beta\big(E_\alpha(X)\big), \tag{75}$$

where E_α denotes Hyperbionic enrichment at strength α and C_β denotes clipping at depth β applied afterward. This licenses a question neither operator can answer alone: which portions of a glyph actually carry recognition, once the reader has other structured cues to draw on? The framework predicts that enrichment can pay for erosion—that

$$C_{0.30}\big(\mathcal{H}(X, p)\big) \tag{76}$$

can be easier to read than

$$C_{0.20}(X), \tag{77}$$

despite retaining physically less of the original glyph, because the prosodic dimensions added by $\mathcal{H}$ supply structured cues that the plain glyph's missing strokes used to supply. Additive and subtractive transformations of the same channel are therefore substitutable, not merely composable: legibility is a function of total available evidence across channels, not of any one channel's completeness.

Progressive clipping also supplies a direct experimental method for locating the *minimal sufficient visual subset* of a word—the smallest fragment of visual evidence a given reader, in a given context, needs to recognize it reliably:

$$V^*(w) \subset V(w) \quad \text{such that} \quad P\big(w \mid V^*(w), \text{context}\big) \geq \tau. \tag{78}$$

Everything outside $V^*(w)$ is, for that reader in that context, perceptually redundant. Clipping words at increasing λ traces a path from ordinary reading, through occasional uncertainty, to probabilistic reconstruction, to something closer to solving a cipher; reversing the process, restoring evidence from a heavily clipped state until a word suddenly "pops" into recognition, locates $V^*(w)$ directly, from the point of collapse rather than the point of failure.

Graphemic Familiarity Versus Typographic Familiarity

A further distinction emerges once clipping is tested across genuinely unfamiliar glyph systems rather than Latin script alone: *graphemic familiarity*, whether a reader knows the individual letterforms, is not the same property as *typographic familiarity*, whether a page carries the statistical geometry of ordinary writing, a stable baseline, a conspicuous height class structure, controlled ascenders and descenders, predictable inter-word spacing, regardless of whether its individual glyphs are legible at all.

$$\text{graphemic familiarity} \neq \text{typographic familiarity}. \tag{79}$$

A script can be built with every character identity unfamiliar while its page-level statistics remain thoroughly familiar, and a reader can register that familiarity, and gain some recognition benefit from it, without being able to name a single letter.

This separates two design axes that are usually conflated: how hard individual glyphs are to identify, and how much second-order structure, the shape of words rather than the shape of letters, survives at the scale of a line or a paragraph.

A family of invented Galactic script variants illustrates the resulting design space directly. Placed side by side, they occupy quite different positions along axes such as

$$\mathcal{T} = (\text{glyph separation},\ \text{height variation},\ \text{baseline regularity},\ \text{stroke continuity},\ \text{word silhouette} \tag{80}$$

with no single dimension from "easy" to "hard" spanning them. A variant that compresses characters into small, similarly weighted marks trades individual-glyph legibility for a kind of paragraph-scale texture; a variant with maximal per-character differentiation trades that texture for strong local identity at the cost of word-level contour; a continuous-stroke cursive variant redistributes identity into directional flow, gaining word rhythm at the price of higher local ambiguity between glyphs sharing a stroke vocabulary; a variant with substantial height and baseline variation retains sequence information below the scale at which individual glyphs resolve; and a variant built from familiar handwriting statistics, ascenders, variable heights, connective rhythm, applied to entirely unfamiliar graphemes can look approachable at a glance precisely because its typographic familiarity is high even though its graphemic familiarity is zero.

Clipping is what turns this design space from a set of categorical comparisons into a continuous one. Applying C_λ within a single variant holds typographic familiarity fixed while varying only the amount of raw evidence available, making it possible to ask, for a fixed script design, exactly how much graphemic evidence a given level of typographic and contextual support can substitute for. This is the same question equation (75) poses for R, run in reverse: not how much structure can be added, but how much can be removed before the invariant underneath the glyph is no longer recoverable.

Legibility is not a property of a glyph. It is a property of the total evidence available for reconstructing it.

Beyond a Single Parameter: A Family of Degradation Operators

Clipping is one member of a much larger family of admissible degradations, and a working implementation of that larger family already exists as a set of geometric transformation operators applied to the carrier fonts themselves rather than to individual clipped glyphs. Where C_λ removes evidence by truncation, this family perturbs glyph geometry continuously: affine and point-noise deformations (jitter, shear, quantize), continuous deformation fields (arch, twist, pinch, fisheye, attractor, vortex), discontinuity-introducing faults (scanlines, split, tectonic), and transformations that move whole contours coherently rather than perturbing unrelated points (memory) or apply nonlinear compression (gravity). A second, more recent suite adds perspective, envelope, fold, fracture, wind, polarization, melt, contour-phase, staircase, and suture operators. Compound multi-stage models combine several of these into a single named progression, `full_decay`, `dissolution`, `wave_erosion`, `geological`, `event_horizon`, `fault_memory`, `crt_failure`, `fossil_compression`, `signal_possession`, each evoking a different physical decay process while remaining, formally, a specific composition of the same primitive operators.

This gives the perturbation family Θ in the robustness measure $\mathcal{R}(Y_i, \Theta)$ of (62) concrete, named populating members rather than the illustrative rotation-and-blur examples used when that measure was first introduced, and it extends the erosion picture of this section past clipping specifically: C_λ deletes evidence outright, while jitter, wave, and the continuous deformation fields relocate it, moving a stroke's information to a nearby but not absent position in the visual field. Both are erosions of $\Delta(g_i)$, the perceptual margin of (65), but they erode it by different mechanisms, and a carrier robust to one need not be robust to the other.

Single-Shot Versus Cumulative Degradation

A further distinction the implementation makes explicit is between two ways of generating a degradation sequence at nominal severities $\lambda_1 < \lambda_2 < \cdots < \lambda_n$. A single-shot sequence applies the operator to the original source at each severity independently,

$$Y_k = C_{\lambda_k}(X), \qquad k = 1, \ldots, n, \tag{81}$$

while a cumulative sequence applies it repeatedly, each state built from its immediate predecessor rather than from X itself,

$$Y_k = C_\delta(Y_{k-1}), \qquad Y_0 = X, \qquad \delta = \lambda_k - \lambda_{k-1}. \tag{82}$$

These need not coincide. If C is idempotent or if its effect on a given glyph saturates, Y_n under (81) and (82) can converge to the same limit; if instead each application introduces its own independent noise or rounding, (82) accumulates error that (81) does not, so that a cumulative sequence at nominal severity λ_n can be substantially more degraded than a single-shot rendering at the same nominal λ_n. Which behavior a given operator exhibits is an empirical question about that operator, not something derivable from its single-application definition alone, which is exactly why the two generation modes are worth keeping distinct in any degradation corpus rather than collapsing them into one λ-indexed family.

Path Dependence and Operator Non-Commutativity

A second empirical question arises once more than one degradation operator is composed. For two operators T_a and T_b, applying a then b need not produce the same result as b then a,

$$T_b \circ T_a(X) \stackrel{?}{=} T_a \circ T_b(X), \tag{83}$$

and whether equality holds is a testable property of the operator pair rather than an assumption a degradation model can make for free. This matters directly for the composed operator $Y_{\alpha,\beta} = C_\beta(E_\alpha(X))$ introduced in (75): if enrichment and erosion fail to commute, the order in which a Hyperbionic field is added and evidence is removed is not a free choice, applying C_β before E_α could leave a different, and possibly more or less legible, result than applying them in the reverse order, and (75)'s particular ordering, clip after enriching, would need to be justified rather than assumed interchangeable with its reverse.

A Caution the Tooling Already Makes Explicit

The implementation's own measurement metadata is careful to label the quantities it records as geometric, contour deviation, coordinate displacement, spatial extent, rather than perceptual or semantic. That caution is worth inheriting explicitly here. The visual metric d used in the collision condition (64) and the margin $\Delta(g_i)$ of (65) are perceptual distances, distances as a reader's visual system weights them, not geometric ones in the sense of raw coordinate difference between two glyph outlines. A large geometric perturbation can leave perceived identity untouched, and a small one can destroy it, exactly the non-linear threshold behavior already noted for λ_i^* in (71). Tooling that measures and logs geometric deformation precisely is a necessary instrument for this research program, since it is what makes the perturbation family Θ reproducible and its severities comparable across experiments, but it is not by itself a measurement of d, and treating geometric distance as a proxy for perceptual distance without validating that proxy against actual reader performance would reintroduce, at the level of the degradation model, the exact conflation this essay has tried to keep apart throughout: what a transformation does to a glyph's coordinates is not the same question as what it does to a reader's ability to recognize it.

Granularity-Controlled Degrading Text

The single-glyph and single-word degradation questions posed throughout this section have a document-scale analogue already implemented: a degradation sequence can be applied to continuous prose at a chosen granularity, a different font from the sequence per paragraph, per sentence, per word, or per page, producing a single document that transitions from an undegraded to a heavily degraded rendering as the reader progresses through it. Word-granularity degradation is the most directly useful of these for the questions raised in Section 13 and Section 12.4: it lets $D_R(T)$ be measured as a function of within-document position rather than only across separate specimens, and it gives production-granularity findings, the index depth $d(x)$ of Section 20's account of ergodic writing, a reading-side counterpart, since a word's recognizability under increasing degradation and a word's retrievability as a production trajectory are, on the account developed in this essay, two faces of the same underlying familiarity variable.

Constraints and Stability

The expressive power of the Hyperbionic system must be bounded to remain usable. Without constraints, the parameter space $\mathbb{R}^m$ allows mappings that render text unreadable—glyphs too small to resolve, rotations that invert letterforms, displacements that destroy word boundaries.

Before developing the formal constraints, it is useful to note that the admissibility problem has a precise analogue in the audio domain. Standard lossy codecs (MP3, AAC) apply a psychoacoustic masking model: when a loud transient such as a snare hit occurs immediately before a quiet signal such as a vocal breath, the algorithm discards the quiet signal on the grounds that the loud event masks it. This produces what audio engineers call *spectral fracturing*: metallic ringing, temporal smearing, and pre-echo artifacts that the auditory system registers subconsciously even when the conscious mind cannot identify them. The computational load of repairing the fractured signal blunts emotional impact.

Spectral fracturing is, in the framework of this paper, a pathological aggregation: a codec that discards masked signal components is a system that factors through a lossy version of $\mathcal{A}$, and by the Aggregation Impossibility Proposition the resulting representation cannot recover expressive coherence χ. What is destroyed is precisely the structured microdynamic jitter that carries the emotional carrier wave—the subtle harmonic weight and temporal micro-variation of a human performance that cannot be reconstructed from amplitude and spectral envelope alone. Hyperbionic rendering must avoid the typographic analogue of spectral fracturing: transformations that preserve nominal glyph structure while destroying the coherence required for perceptual integration. An admissible rendering is one that neither collapses prosodic distinctions nor introduces visual artifacts that impose a reconstruction burden on the reader analogous to the cognitive load of a fractured audio signal. The admissibility constraints introduced informally in Section 4 can be stated precisely.

Define the *perceptual validity region* as the set of parameter vectors p_i such that the rendered glyph $R(g_i, p_i)$ is legible at normal reading distance and reading speed. This region is bounded: there exist maximum and minimum values for each parameter beyond which legibility fails. Within this region, the constraint energy

$$C[p] = \int_{\mathcal{M}} \left(\alpha\, \theta(x)^2 + \beta\, S(x)^2 + \gamma\, \xi(x)^2 \right) d\mu(x) \tag{84}$$

—where θ measures misalignment between the rendering trajectory and the salience gradient, S measures uncertainty in parameter values, and ξ measures rotational instability in the visual field—is bounded above by a legibility threshold $C_{\max}$. Admissible renderings satisfy $C[p] \leq C_{\max}$. The clipping operator of Section 15 is naturally read as extending this same energy with an erosion term: C_λ approaches $C_{\max}$ from below by removing evidence rather than adding it, so admissibility for the destructive dual becomes $C[p] - \lambda \cdot \Xi(g) \geq C_{\min}$ for a legibility floor $C_{\min}$, with Ξ measuring the visual salience removed at depth λ. Enrichment and erosion are therefore two directions of motion within one constraint energy, not two separate design problems.

The legibility constraint has a further consequence: it implies that Hyperbionic rendering operates on a low-dimensional admissible manifold within the full parameter space. Not all combinations of the parameters in (12) are jointly admissible; the constraints couple the parameters and restrict the system to a structured subset of $\mathbb{R}^m$. This is the typographic analogue of the biological prior in cognitive trajectory models: the system does not search the full parameter space uniformly but is confined by legibility and stability constraints to a lower-dimensional structured region.

The perceptual weights w_i in the G-metric are not universal but listener-variable. A relevant empirical observation is that audiometric studies have reported that women, on average, exhibit approximately 2 dB greater sensitivity than men across frequency ranges, a difference attributed to evolutionary pressures related to detecting the high-frequency cues of infant distress. If this differential sensitivity is real and of the reported magnitude, it has a direct consequence for spectral fracturing: compression artifacts that fall below the conscious detection threshold of a less sensitive auditory system may register supra-threshold for a more sensitive one, imposing a subconscious cognitive load on the listener that blunts emotional impact. In the framework of this paper, this corresponds to listener-specific G-metrics with higher weights on the dimensions most affected by compression artifacts—temporal fine structure and high-frequency harmonic content. A Hyperbionic rendering system that aims to preserve emotional impact across a diverse listener population must therefore parameterize G as a function of the target perceptual profile, not treat it as a fixed universal constant. The claim about 2 dB differential sensitivity is taken from existing discourse on this topic and should be understood as an empirical hypothesis requiring controlled audiometric validation rather than an established universal constant; the structural point about listener-variable G-metrics holds independently of the specific magnitude. The system must therefore treat G as a parameterized perceptual model rather than a fixed metric, adapting the weighting structure to the sensitivity profile of the target observer.

Implementation: The Marine Processor as $\mathcal{M}$ in Practice

The measurement operator $\mathcal{M}$ defined in Section 2 is not merely a formal object. It has a concrete, running implementation in the Marine processor, a Rust library designed for $O(1)$ per-sample operation. Examining the implementation reveals three places where the formal definition and the executable code diverge in instructive ways, and one where the implementation makes a stronger architectural commitment than the formalism requires.

Exponential Moving Average versus Window Mean

The formal definition of period jitter uses sample means: $j_p(k) = |\Delta t_k - \overline{\Delta t}|/\overline{\Delta t}$, where $\overline{\Delta t}$ is the mean inter-peak interval over all observed peaks. This is clean mathematically but impractical for real-time processing, since computing the sample mean requires storing all past periods and updating a running sum—operations that are $O(N)$ in memory if not time.

The implementation replaces the sample mean with an exponential moving average (EMA). Let μ_k denote the EMA of inter-peak periods after the k-th peak. The update rule is

$$\mu_k = \alpha_p \cdot \Delta t_k + (1 - \alpha_p) \cdot \mu_{k-1}, \tag{85}$$

where $\alpha_p \in (0, 1)$ is the EMA smoothing coefficient configured at initialization. Jitter is then computed as $j_p(k) = |\Delta t_k - \mu_{k-1}|/\mu_{k-1}$, using the previous EMA value as the reference rather than the global mean. An identical EMA μ_k^a tracks peak amplitudes for the amplitude jitter computation.

The classical definition of jitter assumes a stationary reference distribution. This assumption is violated in natural speech, where fundamental frequency drifts continuously over time. The EMA formulation replaces a global reference with a locally adaptive one, allowing the system to track prosodic intent rather than penalize it as deviation. The substitution is therefore not an optimization but a correction to the measurement model itself: the formal definition in equation (9) should be read as using a weighted mean with exponential decay rather than a uniform sample mean. A speaker who gradually lowers their pitch will show low EMA-based jitter throughout, correctly identifying the signal as locally periodic despite global drift; the sample-mean version would misclassify the drift as instability.

The EMA also implements the warmup condition implicitly. The processor exposes an `is_warmed_up()` predicate that returns true only when at least three peaks have been detected and the EMA has received enough updates to be reliable. Formally, this means that $\mathcal{M}(u)$ is a partial function: it is undefined on waveforms too short to contain at least three peaks satisfying the minimum period constraint. The sliding window $\gamma(t) = \mathcal{M}(u \restriction_{[t-\Delta,t]})$ introduced in Section 7 therefore requires a window width Δ satisfying

$$\Delta \geq \frac{3}{f_0}, \tag{86}$$

where f_0 is the fundamental frequency of the signal. For speech at 100–300 Hz, this constrains $\Delta \geq$ 10–30 milliseconds—a natural lower bound that the implementation enforces implicitly through the warmup predicate.

The Harmonic Coherence Placeholder

The formal vector (9) includes a harmonic coherence component h measuring the degree of periodic regularity in the voiced signal. In the current implementation, this component is hardcoded to $h = 1.0$ with a comment marking it as a TODO item: "Harmonic score (simplified – TODO: FFT-based detection). For now, assume voiced content."

This means the implementation currently computes a seven-dimensional effective vector, not an eight-dimensional one. The eighth dimension—harmonic coherence—is present structurally but carries no information. The salience score $s = 1/(1 + \overline{j_p} + \overline{j_a})$ is consequently computed from jitter alone, without any contribution from spectral periodicity. Signals with strong harmonic structure (sustained vowels) and signals with weak harmonic structure (fricatives, noise) receive the same h value and are distinguished only by their jitter profiles.

The intended extension is FFT-based harmonic detection: computing the ratio of energy at the fundamental frequency and its harmonics to total signal energy, which gives a value in $[0, 1]$ that approaches 1 for purely periodic signals and 0 for white noise. Formally,

$$h = \frac{\sum_{k=1}^{K} |U(kf_0)|^2}{\int_0^{f_s/2} |U(f)|^2 \, df}, \tag{87}$$

where $U(f)$ is the discrete Fourier transform of a windowed segment of $u(t)$, f_0 is the estimated fundamental frequency, and K is the number of harmonics included. This computation is $O(N \log N)$ per window rather than $O(1)$ per sample, which is why it has not yet been integrated: it would require a hybrid architecture in which the peak-based $O(1)$ processor feeds a periodic FFT-based harmonic estimator operating on a longer lookback buffer.

The formal framework anticipates this extension naturally. The measurement operator $\mathcal{M}$ is defined abstractly as a map to $\mathbb{R}^n$; the specific components are a concrete instance, not a structural constraint. Adding a genuinely computed h component does not change the architecture of the Hyperbionic system—the equivalence (15) holds for any prosodic parameter vector, regardless of dimensionality—but it does change the information content of the modal coordinate Z_α and therefore the discriminative power of the trajectory resonance recognizer. Utterances that are currently indistinguishable (same jitter profiles, different harmonic structure) would become distinguishable once h is measured rather than assumed. Until this component is implemented, the system operates in a reduced discriminative regime in which periodicity is inferred indirectly through jitter rather than measured explicitly. This is a structural limitation of the current implementation, not merely an engineering detail.

Operational Constraints and Real-Time Geometry

The Marine processor enforces two further constraints that have formal analogues in the measurement operator's domain of definition: a period validity gate and a clip threshold.

Period Validity Gate

The processor accepts a peak contribution only when the inter-peak period falls within a configurable range [`min_period`, `max_period`] specified in samples. This gate serves two purposes: it excludes spurious detections (very short periods corresponding to noise spikes) and it excludes silence gaps (very long periods corresponding to pauses between utterances). Formally, let f_s denote the sample rate. The gate defines an admissible frequency range

$$f_{\min} = \frac{f_s}{\texttt{max\_period}}, \qquad f_{\max} = \frac{f_s}{\texttt{min\_period}}, \tag{88}$$

and the measurement operator is defined only on signal segments whose instantaneous fundamental frequency lies within $[f_{\min}, f_{\max}]$. For the default speech configuration at 22050 Hz, typical values confine the operator to voiced fundamental frequencies in the speech range, rejecting both subsonic artifacts and aliased high-frequency noise.

The period gate has a geometric interpretation in trajectory space. A trajectory $\Gamma = \{Z_\alpha(t_k)\}$ is defined only at time steps where a valid peak is detected within the admissible period range. At time steps where the signal is silent, unvoiced, or outside the frequency range, the trajectory is undefined—the point is simply absent from the sequence. This means that word basins $\mathcal{W}_i$ are sparse trajectories: sequences of modal coordinates at the times of valid peaks, with gaps corresponding to unvoiced or silent intervals. The DTW coherence functional (27) must be understood as aligning sparse sequences, not dense time series, which the standard DTW algorithm handles naturally through its admissible alignment path constraint.

Clip Threshold as a Pre-Gate

Before any peak detection is attempted, the processor applies a clip threshold: samples with absolute value below `clip_threshold` are ignored entirely, bypassing even the peak detection logic. This is a pre-gate that defines the silence floor of the system.

Formally, let $\varepsilon_{\text{clip}} > 0$ denote the clip threshold. The effective input to $\mathcal{M}$ is not $u(t)$ itself but the gated signal

$$u_\varepsilon(t) = \begin{cases} u(t) & \text{if } |u(t)| \geq \varepsilon_{\text{clip}}, \\ 0 & \text{otherwise.} \end{cases} \tag{89}$$

The measurement operator $\mathcal{M}$ acts on u_ε, not on u. This means that very quiet passages—below the noise floor of the recording environment—contribute no peaks and no trajectory points. The clip threshold is therefore the operational definition of silence in the Marine framework: a continuous segment on which $u(t)$ lies entirely below $\varepsilon_{\text{clip}}$ produces no output from $\mathcal{M}$, and its absence from the trajectory is the signal that a silence or unvoiced interval has occurred.

In the Hyperbionic context, this gating has a direct typographic correlate. Tokens in a transcript that correspond to silent intervals—pauses, breaths, hesitations—receive no prosodic parameter vector from $\mathcal{M}$, and so their Hyperbionic rendering falls back to the default glyph $R(g_i, \mathbf{0})$: unstyled, unmodified text. Silence becomes the absence of typographic transformation, which is the correct rendering: a pause in speech is marked in Hyperbionic text by the surrounding white space, not by any active visual property of the adjacent glyphs.

Beyond the Audible-Stable Regime: Haptic Extension and Expressive Deviation

This section removes two simplifying assumptions of the preceding framework: that all relevant structure lies within the audible band, and that deviation from periodicity is noise. Both assumptions exclude meaningful signal. The extensions introduced here incorporate sub-audible somatic structure and reinterpret deviation as a carrier of intention, completing the invariant field.

The formulation developed thus far assumes that prosodic structure is captured by stable periodic features within the audible frequency band. This assumption is both physically and perceptually incomplete in two orthogonal directions. First, acoustic signals below approximately 40 Hz are not primarily perceived auditorily but somatically, as vibration felt in the chest, body, and surrounding environment. Second, the salience formula $s = 1/(1 + \overline{j_p} + \overline{j_a})$ treats all jitter as degradation, which is correct for detecting synthetic or damaged signals but wrong for expressive performance, where controlled deviation is the carrier of meaning. What was previously classed as noise occupies exactly the dimensions where intention lives.

Infrasound and the Haptic Channel

The Marine configuration gates the measurement operator to an admissible frequency range $[f_{\min}, f_{\max}]$ corresponding to roughly 60–4000 Hz for speech. Signals below $\sim$ 40 Hz are discarded. But low-frequency content below the auditory threshold is not absent from musical and environmental signals: the sub-bass of a bass guitar, the chest-felt pulse of a kick drum, the room pressure of a large acoustic space are all real physical quantities that carry structural information about the source and environment.

Let $u(t)$ be decomposed spectrally into

$$u(t) = u_{\text{aud}}(t) + u_{\text{infra}}(t), \tag{90}$$

where u_{infra} contains components with instantaneous frequency $f < 40$ Hz. The current measurement operator $\mathcal{M}$ acts only on u_{aud}. We define the extended measurement operator

$$\widetilde{\mathcal{M}}(u) = \big(\mathcal{M}(u_{\text{aud}}),\ H(u_{\text{infra}})\big), \tag{91}$$

where H is a *haptic measurement functional* extracting the low-frequency envelope:

$$H(u_{\text{infra}}) = \big(A_{\text{lf}},\ \sigma_{\text{lf}},\ \nabla A_{\text{lf}}\big). \tag{92}$$

Here A_{lf} is the low-frequency energy envelope, σ_{lf} its temporal variance, and ∇A_{lf} its rate of change. These quantities encode perceived pressure, pulsation rate, and environmental resonance—the somatic correlates of musical bass.

The haptic channel is structurally distinct from the auditory channel in two respects. Perceptually, infrasound is field-like: it is felt across the whole body rather than localized in the auditory system, and the relevant spatial scale is the body or room rather than the cochlea. This means that in the Hyperbionic rendering, infrasound does not map to glyph-level deformation but to *global layout modulation*—baseline drift, field-wide spacing variation, or background texture—reflecting the distributed rather than localized nature of somatic perception. Formally, the trajectory space extends to $V = \mathbb{R}^{8+3}$, with the three haptic dimensions decoupled from the G-metric of the auditory dimensions and requiring separate perceptual weighting.

Structured Jitter as Expressive Signal

Jitter, in the current framework, is defined as deviation from an exponentially weighted expected period. But this definition conflates two categorically different phenomena. Random jitter arises from measurement noise, imprecise articulation, or signal degradation: it has no temporal structure and carries no information beyond the degradation level. Structured jitter arises from intentional expressive modulation: vibrato in a sustained note is periodic jitter; groove in a rhythm section is timing jitter locked to a metrical grid; the roughness of a distorted guitar is amplitude jitter with a specific spectral signature. These are not corruptions of a periodic signal but features of it.

We decompose the observed jitter sequence $\{j(k)\}$ into two components:

$$j(k) = j_{\text{rand}}(k) + j_{\text{expr}}(k), \tag{93}$$

where j_{rand} is stochastic and carries no predictive structure, and j_{expr} is structured, reproducible, and carries expressive information.

Definition 1 (Expressive Coherence). *Let* $\{j(k)\}_{k=1}^{N}$ *be a sequence of jitter measurements and* $\{\hat{j}(k)\}$ *a locally predicted sequence obtained by fitting a short-memory model to recent values. The* expressive coherence *is*

$$\chi = 1 - \frac{\mathrm{Var}\big(j(k) - \hat{j}(k)\big)}{\mathrm{Var}\big(j(k)\big)}, \tag{94}$$

with $\chi \in [0, 1]$*:* $\chi \approx 1$ *when deviation follows a predictable pattern,* $\chi \approx 0$ *when deviation is indistinguishable from white noise.*

High χ at substantial $\bar{j}$ indicates expressive performance. Low χ at substantial $\bar{j}$ indicates damage or noise. Low χ at low $\bar{j}$ indicates a synthetic or mechanically regular signal. The original scalar salience s cannot distinguish the first from the third of these cases when mean jitter happens to be comparable; the expressive coherence χ distinguishes all three.

We define a second salience axis

$$s_{\mathrm{expr}} = \chi \cdot (\overline{j_p} + \overline{j_a}), \tag{95}$$

measuring the magnitude of structured deviation: it is large when jitter is both substantial and organized. The full salience representation is then two-dimensional:

$$\mathbf{s} = (s_{\mathrm{stable}}, \; s_{\mathrm{expr}}), \tag{96}$$

where $s_{\mathrm{stable}} = s = 1/(1 + \overline{j_p} + \overline{j_a})$ is the existing periodicity salience and s_{expr} is the new expressive axis. Stable periodic signals maximize s_{stable}; expressive signals maximize s_{expr}; synthetic or damaged signals minimize both.

The two-dimensional salience space has an important application to the authentication of human performance. A human vocal performance is produced by a coupled physical system: lungs, diaphragm, vocal cords, resonant cavities, and neural motor control all constrain the jitter profile jointly. The resulting jitter is not random but structured by physiology—it lies near the constraint manifold of a biological dynamical system. We call this property *biological coupling*: the jitter sequence is organized by a physical process that imposes internal consistency across time scales from milliseconds (glottal pulse variation) to seconds (respiratory cycle). Generative audio synthesis systems, by contrast, produce jitter by sampling from learned distributions over spectral and temporal features. The resulting jitter is *decoupled*: it may match the marginal statistics of human jitter (mean, variance, spectral envelope) while failing to reproduce the coupled temporal structure. In the framework of this paper, biological coupling corresponds to high χ with a structured manifold, while decoupled synthetic jitter produces low

χ despite superficially plausible amplitude and pitch.

Proposition 3 (Biological Coupling Detectability). *Let u_{human} be a human vocal performance and u_{synth} a generative synthesis of the same utterance. If the synthesis system matches the aggregate statistics $\mathcal{M}(u_{\text{human}}) \approx \mathcal{M}(u_{\text{synth}})$ but does not model the physiological coupling of the human jitter process, then $\chi(u_{\text{human}}) \gg \chi(u_{\text{synth}})$ and the two signals are distinguishable by trajectory coherence even when indistinguishable by aggregate prosodic statistics.*

This proposition provides the mathematical basis for biometric voice authentication via expressive coherence: the structured biological jitter of a human performance is not merely a stylistic feature but a physically grounded invariant that aggregate-matching synthesis cannot replicate without modeling the underlying physiology. This establishes a separation principle: synthesis systems that match marginal statistics but fail to reproduce coupled temporal structure remain distinguishable under trajectory-based metrics. A voice authentication system based on χ is therefore resistant to attacks that match spectral envelope, pitch contour, and mean jitter while lacking the physiological coupling that generates structured temporal coherence in human performance.

Proposition 4 (Aggregation Information Loss). *The aggregation map $\mathcal{A}$ is not injective on trajectories: $\mathcal{A}(\Gamma_1) = \mathcal{A}(\Gamma_2)$ does not imply $\Gamma_1 = \Gamma_2$. Therefore any system that operates exclusively on $\mathcal{M}(u) = \mathcal{A}(\{\mathcal{P}_k\})$ cannot recover trajectory curvature or expressive coherence χ.*

This is not a limitation of any particular model design but a general impossibility result for the class of representations that factor through $\mathcal{A}$. Standard acoustic embedding systems, which map utterances to fixed-length vectors derived from averaged or pooled features, belong to this class. The trajectory-based architecture proposed here does not factor through $\mathcal{A}$, and so is not subject to this limitation.

Reinterpretation of Annotated Noise in TARTAN

Under the original formulation, the annotated noise field $\eta_{\ell,j}$ in each TARTAN tile records structured deviation to be tracked and, implicitly, suppressed or normalized away. The decomposition (93) and the expressive coherence (94) permit a more discriminating treatment. Each tile is extended to

$$\tau_{\ell,j} = \left(\bar{Z}_{\ell,j},\ \Sigma_{\ell,j},\ \eta_{\ell,j},\ \chi_{\ell,j},\ b_{\ell,j}\right), \tag{97}$$

where $\chi_{\ell,j}$ is the expressive coherence computed over the packets within tile (ℓ, j). The noise field $\eta_{\ell,j}$ and coherence $\chi_{\ell,j}$ together classify tile content:

$$\begin{aligned} \eta \approx 0,\ \chi \approx 0 \ &\Rightarrow\ \text{silence or highly stable signal,} \\ \eta > 0,\ \chi \approx 0 \ &\Rightarrow\ \text{noise or damaged signal,} \\ \eta > 0,\ \chi \approx 1 \ &\Rightarrow\ \text{expressive signal.} \end{aligned} \tag{98}$$

This classification replaces the binary noise/signal distinction with a ternary structure that can represent the full range from mechanical precision through expressive performance to genuine noise—three regimes that were previously conflated whenever mean jitter values happened to agree.

Example: Robotic versus Expressive Utterance

To make the extended framework concrete, consider two realizations of the same lexical item that are indistinguishable under aggregate prosodic statistics but distinguishable under the expressive axis.

Let $u_{\text{robot}}(t)$ be a synthesized utterance with perfectly regular timing and amplitude, and $u_{\text{expr}}(t)$ a human-performed utterance with controlled vibrato. Both may yield similar aggregate vectors: $\mathcal{M}(u_{\text{robot}}) \approx \mathcal{M}(u_{\text{expr}})$ when mean jitter and energy are comparable over the full utterance.

At the packet level, however, the two signals differ structurally. The robotic jitter sequence satisfies

$$j_{\text{robot}}(k) \approx \varepsilon_k, \qquad \chi_{\text{robot}} \approx 0, \tag{99}$$

where ε_k is small unstructured noise. The expressive jitter sequence satisfies

$$j_{\text{expr}}(k) = A \sin(\omega k) + \varepsilon_k, \qquad \chi_{\text{expr}} \approx 1, \tag{100}$$

with structured vibrato at frequency ω and amplitude A. The two-axis salience representation then yields

$$\begin{aligned} \mathbf{s}_{\text{robot}} &= (s_{\text{stable}} \approx 1,\ s_{\text{expr}} \approx 0), \\ \mathbf{s}_{\text{expr}} &= (s_{\text{stable}} < 1,\ s_{\text{expr}} \approx 1). \end{aligned} \tag{101}$$

At the trajectory level, both utterances trace paths $\Gamma_{\text{robot}}, \Gamma_{\text{expr}} \subset \mathbb{R}^8$ with similar global positions but different local curvature. The expressive trajectory exhibits coherent oscillation in the jitter dimensions; the robotic trajectory remains nearly linear. Under the G-weighted coherence functional (29), where jitter dimensions carry higher weight,

$$\mathcal{C}(\Gamma_{\text{expr}}, \Gamma_{\text{expr}}) \gg \mathcal{C}(\Gamma_{\text{expr}}, \Gamma_{\text{robot}}), \tag{102}$$

despite similarity in aggregate statistics. The system recognizes the expressive utterance as self-similar and the robotic utterance as structurally distinct from it, even when both are correctly identified as the same word by the stability coherence.

This example demonstrates a structural claim about where meaning lives:

$$\text{meaning} = (\text{location}, \text{curvature}, \text{coherence}). \tag{103}$$

$$\textbf{meaning} = (\textbf{location}, \textbf{curvature}, \textbf{coherence})$$

Definition 2 (Semantic Decomposition)**.** *The meaning of a prosodic signal is fully specified by three components: its position in parameter space* (V, G) *(location), its temporal evolution through that space (curvature), and the structural organization of that evolution (coherence). No component is recoverable from the others.*

Traditional prosodic analysis captures location alone—position in feature space averaged over the utterance. Trajectory analysis adds curvature—the local geometry of motion through that space. Expressive coherence adds the third dimension: whether the curvature is organized or random. The three components are jointly necessary: location without curvature cannot distinguish a word from a sustained tone; curvature without coherence cannot distinguish expression from damage; coherence without location cannot ground meaning in a specific region of the invariant space. Without all three, the system cannot distinguish intention from noise.

Trajectory Regimes and Ergodic Writing Dynamics

This section formalizes an observed phenomenon in human writing systems: the switching between continuous and discrete inscription modes—cursive versus print, gesture input versus letter-by-letter typing. We show that this switching is governed by trajectory predictability and corresponds to an ergodic exploration of modal space, directly instantiating the word basin architecture of Section 26. Hyperbionic rendering makes this latent control variable explicit as a typographic invariant.

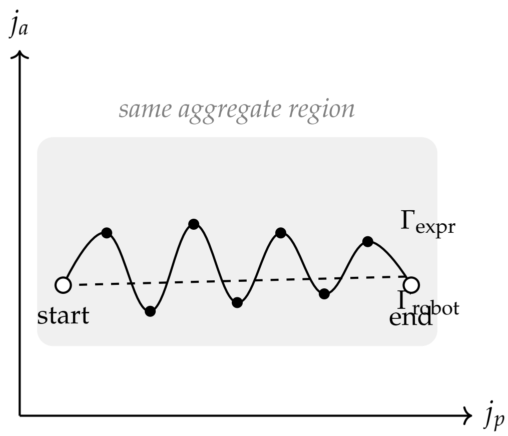

Figure 3: Two utterances of the same word occupy the same aggregate region of prosodic space (shaded) but differ in trajectory geometry. The robotic signal (dashed) follows a near-linear path; the expressive signal (solid) exhibits structured oscillation in the jitter dimensions, with dots indicating individual salience packet samples. Trajectory curvature and expressive coherence χ distinguish the two signals; aggregate statistics alone do not.

Two Inscription Regimes

Human writing systems exhibit two dynamically distinct regimes of trajectory production. Cursive handwriting, swipe-based keyboard input, and fluent motor execution form the *continuous regime* Γ_{cont}: low segmentation, smooth curvature, high coherence, and a single motor plan executed without inter-symbol resets. Printed handwriting, letter-by-letter typing, and deliberate construction form the *discrete regime* Γ_{disc}: explicit segmentation, piecewise structure, and a separate motor plan per glyph.

These regimes are not stylistic choices. They are dynamical responses to the predictability of the underlying trajectory. Writers spontaneously switch from cursive to print when encountering an unfamiliar or ambiguous word, and revert to cursive once familiarity is restored. The same behaviour appears in trace-based mobile keyboards: a common word is entered as a single continuous swipe gesture (trajectory collapse onto a stored basin); an unknown or ambiguous word forces discrete letter-by-letter entry. The switching is governed by the same mechanism in both cases, and that mechanism is local uncertainty about trajectory continuation.

A useful refinement of this picture asks not merely whether a sequence is retrieved as a stable unit, but at what grain it is retrieved. Define the *index depth* of a symbolic sequence x as

$$d(x) = \max\{k : x \text{ can be retrieved as a stable unit at level } k\}, \tag{104}$$

over an ordered family of representational scales

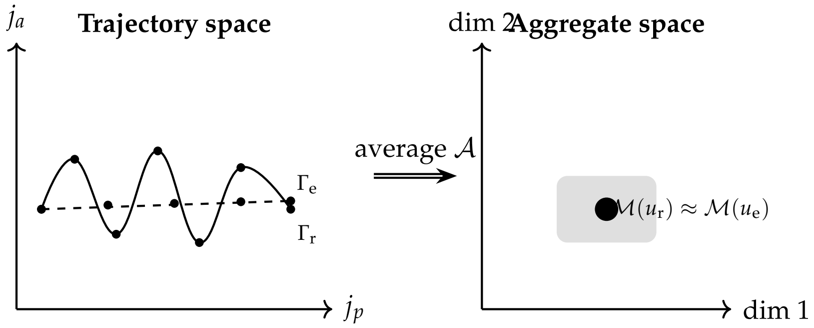

Figure 4: Failure mode of aggregate-only analysis. In trajectory space (left), the robotic path Γ_r (dashed) and expressive path Γ_e (solid) are geometrically distinct. After averaging via $\mathcal{A}$ (right), both collapse to the same region of aggregate feature space, making them indistinguishable. Expressive coherence χ and trajectory-level DTW are required to recover the distinction.

$$\mathcal{U} = \{\text{stroke, grapheme, cluster, morpheme, word, phrase, construction}\}. \tag{105}$$

An unfamiliar sequence, a postal code, a neologism, collapses toward the finest levels of $\mathcal{U}$; a heavily practiced phrase can be retrieved as a single unit near the coarsest level, without its component words being separately accessed. Index depth is not fixed for an utterance as a whole: it varies continuously across production, $d(t)$, entering and leaving basins as familiar and unfamiliar material alternate, which is exactly the mixed cursive/print behaviour observed within a single sentence.

Predictability and Regime Selection

Let H_i denote the local continuation entropy at token T_i, defined as

$$H_i = -\sum_j P\big(\Gamma_{i+1} = j \mid \Gamma_{\le i}\big) \log P\big(\Gamma_{i+1} = j \mid \Gamma_{\le i}\big). \tag{106}$$

The observed writing behaviour defines an implicit *trajectory regime selector*:

$$\mathcal{R}(H_i) = \begin{cases} \Gamma_{\text{cont}} & \text{if } H_i < \tau, \\ \Gamma_{\text{disc}} & \text{if } H_i \ge \tau, \end{cases} \tag{107}$$

where τ is a threshold set by motor and cognitive constraints. Below threshold, continuation is sufficiently predictable that the trajectory can be executed as a single motor plan; the writer does not need to specify each symbol explicitly. Above threshold, continuation is ambiguous and the trajectory must be constructed symbol by symbol.

Proposition 5 (Predictability–Continuity Correspondence)**.** *Low-entropy trajectory regions admit continuous motor execution; high-entropy regions require discrete reconstruction. The transition is governed by* $\mathcal{R}(H_i)$*.*

The formal and semantic connotations of the two regimes differ because they carry different trajectory information. Cursive encoding is used for well-integrated, frequently traversed paths and carries a signal of fluency, familiarity, and register; printed encoding is used for careful specification and carries a signal of precision, formality, or uncertainty. These are not arbitrary conventions but consequences of the underlying trajectory structure: continuous flow through a high-density basin versus discrete construction outside one.

Word Basins and Ergodic Writing

The regime selection connects directly to the word basin architecture of Section 26. Let $\mathcal{B} \subset V$ denote a word basin—a high-density region of modal space corresponding to a frequently produced trajectory. Then:

$$\Gamma \in \mathcal{B} \;\Rightarrow\; \Gamma \approx \Gamma_{\text{cont}}, \qquad \Gamma \notin \mathcal{B} \;\Rightarrow\; \Gamma \approx \Gamma_{\text{disc}}. \tag{108}$$

Over extended writing, the process alternates between continuous traversal of high-density basins and discrete exploration of low-density regions. This alternation constitutes an ergodic sampling of trajectory space. A word's basin is built by exactly this repetition: with enough accumulated realizations $\Gamma_w^{(1)}, \Gamma_w^{(2)}, \ldots$ of a word w, a temporal average over one's own past productions comes to approximate the ensemble of admissible realizations of w,

$$\frac{1}{T}\sum_{t=1}^{T} f\big(\Gamma_w^{(t)}\big) \;\longrightarrow\; \mathbb{E}_{\Gamma\sim\mathcal{B}(w)}\big[f(\Gamma)\big], \tag{109}$$

which licenses launching the whole trajectory rather than reconstructing it letter by letter. This is *ergodic substitution*: personal history standing in for an ensemble that was never sampled directly. The claim should be read narrowly: it is not that a word's production process is globally ergodic in the strict sense, natural language exposure is nonstationary, a speaker's vocabulary and register shift over years, and no word is produced under conditions stable enough to license that stronger reading, but that (109) holds as a local approximation, valid over the timescale and context in which w's recent realizations were actually sampled. *Ergodic depth* is accordingly the largest scale in $\mathcal{U}$ at which this local approximation currently holds for a given individual, not a fixed property of the word itself. A neologism or an arbitrary string such as a postal code has no such history, $\rho(c_1 \cdots c_n) \approx 0$ even when every individual character is maximally familiar, $\rho(c_i) \gg 0$, so production has no basin to fall back on and must decompose:

$$\text{novel sequence} \xrightarrow{\text{decompose}} \{\text{well-sampled subtrajectories}\} \xrightarrow{\text{execute}} \text{written form.} \tag{110}$$

With repetition the boundary of decomposition moves upward, letters fusing into digraphs, digraphs into the whole word, as the word accumulates its own sampled history and becomes ergodic in the sense of (109).

Definition 3 (Ergodic Writing Process)**.** *A writing process is* ergodic over trajectory space *if, over time, it samples both high-density (continuous) and low-density (discrete) regions of V, with transitions governed by local predictability H_i.*

Ergodicity in this sense is not a metaphor: it means that the full modal space is eventually traversed by any sufficiently productive writer, with the density of traversal reflecting the frequency distribution of encountered trajectories. Frequently written words accumulate dense basins and are executed continuously; rare or technical words are constructed discretely each time, gradually building thinner basins through repetition. Index depth and basin density are two descriptions of the same fact: $d(x)$ is high exactly where x's basin is dense enough to sustain ergodic substitution, and low exactly where it is not.

Gesture Input as Trajectory Collapse

Swipe-based keyboards instantiate the same regime selection digitally. A gesture Γ_{in} is matched against stored word basins $\{\mathcal{W}_i\}$ via the coherence functional:

$$\hat{i} = \arg\max_i \, \mathcal{C}_{\text{DTW}}(\Gamma_{\text{in}}, \mathcal{W}_i), \tag{111}$$

with acceptance if $\mathcal{C}_{\text{DTW}} > \theta$. If no basin exceeds threshold, the system declines to resolve the gesture and prompts discrete letter entry. This is structurally identical to the regime selector (107): ambiguity forces discretization, and the threshold θ plays the same role as τ.

Proposition 6 (Trajectory Collapse Condition)**.** *Continuous gesture input is admissible if and only if the incoming trajectory collapses onto a unique basin under the DTW coherence functional* (111)*. Otherwise, discrete specification is required. The admissibility condition is the digital analogue of handwriting regime selection.*

The connection to the biological coupling proposition is immediate: gesture input systems that model the trajectory rather than the symbol sequence are, by the same argument, more robust to ambiguity and more sensitive to expressive variation. A swipe keyboard that tracks jitter coherence χ in the gesture would distinguish deliberate slow tracing (high χ, low H) from rapid ambiguous sweeping (low χ, high H) and apply different recognition strategies accordingly.

Hyperbionic Rendering of Trajectory Regimes

The regime structure is a latent invariant of natural writing that conventional typography discards: plain text makes no distinction between a word entered with high fluency and one laboriously constructed. Hyperbionic rendering makes this invariant explicit by extending the parameter vector p_i with a continuity parameter c_i derived from predictability:

$$c_i = \exp(-\lambda H_i) \;\in\; (0,1], \tag{112}$$

where $\lambda > 0$ scales the sensitivity to entropy. The rendering operator R maps c_i to typographic continuity:

$$\begin{aligned} c_i \to 1 \;&\Rightarrow\; \text{smooth, connected glyph flow (continuous regime),} \\ c_i \to 0 \;&\Rightarrow\; \text{segmented, discrete glyph rendering (discrete regime).} \end{aligned} \tag{113}$$

Continuity is a visible invariant of predictability.

This makes explicit what is implicit in handwriting: the degree to which a trajectory is known in advance becomes a visual property of the rendered text. A reader encountering a word rendered in high-continuity mode receives a signal not only about its prosodic structure but about its familiarity in the producing context—the typographic equivalent of the cursive encoding of fluency.

Proposition 7 (Regime Invariance)**.** *Trajectory regime (continuous versus discrete) is an invariant under admissible projection. Any representation that collapses regime distinctions discards information about predictability, ergodic position in trajectory space, and cognitive load. Plain text collapses this invariant; Hyperbionic text preserves it.*

The continuity parameter c_i is co-registered with the expressive coherence χ: high χ with high c_i indicates fluent expressive performance; high χ with low c_i indicates controlled expressive production in an unfamiliar register; low χ with high c_i indicates fluent but metrically regular output; low χ with low c_i indicates constructed, noise-dominated signal. These four regimes correspond to distinguishable positions in the joint salience space $(\mathbf{s}, c_i)$ and admit different rendering strategies.

Fluency is not only speed; it is continuity of trajectory through known space.

Experimental Prediction: Keyboard Layout Transfer and Basin Depth

The ergodic writing framework generates a falsifiable prediction that can be tested without specialised equipment. Consider a participant whose dominant layout is QWERTY. When transcribing on a non-dominant layout such as Dvorak, the familiar motor trajectories for common words are no longer available as continuous stored plans: the key positions differ, so the motor basin has different coordinates in the new layout's parameter space. The participant must reconstruct each word more explicitly.

The prediction is that this transfer cost is not uniform across words. Let $t(w, L)$ denote the time to produce word w on layout L. A linear model gives

$$t(w, L) = \alpha_L \cdot n(w) + \beta_L \cdot H(w) + \varepsilon, \tag{114}$$

where $n(w)$ is word length, $H(w)$ is the continuation entropy (unfamiliarity) of the word, and α_L, β_L are layout-specific coefficients. The core prediction is:

$$\beta_{\text{Dvorak}} > \beta_{\text{QWERTY}}, \tag{115}$$

for a QWERTY-dominant participant. Unfamiliar words, which require letter-by-letter reconstruction regardless of layout, incur a disproportionately larger latency penalty under the non-dominant layout because familiar words have motor basins in QWERTY space that partially transfer (via shared ergodic structure), while unfamiliar words have no such basins in either layout and must be constructed from scratch in a space the participant does not know. The ratio β_L/α_L measures how much worse entropy is relative to length in each layout: a higher ratio under Dvorak confirms that trajectory basin depth, not raw length, is the primary determinant of non-dominant layout cost.

Proposition 8 (Differential Transfer Prediction)**.** *Under the ergodic writing model, the latency penalty for unfamiliar words under a non-dominant keyboard layout exceeds the penalty for familiar words by an amount proportional to the depth of the motor basin deficit:* $\beta_{\text{Dvorak}} - \beta_{\text{QWERTY}} \propto \Delta_{\text{basin}}$*, where* Δ_{basin} *measures the average difference in basin density between the two layouts for the word set.*

The same prediction extends to gesture-based input. On a swipe keyboard, words for which the participant has a stable continuous gesture should transfer poorly to an unfamiliar layout (because the spatial gesture path changes), while words that were always typed discretely should transfer approximately equally. This distinguishes two populations of words in any individual's writing: those stored as continuous motor trajectories (basin residents) and those always constructed symbol by symbol (basin non-residents).

Variational Reconstruction Principle

The persistence and RSVP interpretations of the preceding sections suggest a compact variational principle that unifies the entire pipeline. The RSVP field does not merely evolve by local update rules; it evolves toward configurations that maximize stable reconstructibility across admissible projections. This section states that principle precisely and shows that Hyperbionic rendering is its typographic instantiation.

Let $X(t) = (\Phi(t), \mathbf{v}(t), S(t))$ denote the RSVP field state, and let $\{\mathcal{P}_k\}_{k=1}^{K}$ be a family of projection operators into observable media: acoustic signal, modal memory, typographic rendering, motor gesture, and contextual markup. A configuration is admissible when its projections remain mutually reconstructible.

Define the reconstruction loss

$$\mathcal{R}[X] = \sum_{k,\ell} \int_0^T d_k(\mathcal{P}_k(X(t)),\ \mathcal{T}_{k\ell}\,\mathcal{P}_\ell(X(t)))^2\,dt, \tag{116}$$

where d_k is the metric in the k-th observation space and $\mathcal{T}_{k\ell}$ is the translation operator from modality ℓ to modality k. This term penalises disagreement between different renderings of the same underlying field. The total action is

$$\mathcal{A}[X] = \int_0^T \mathcal{L}_{\mathrm{RSVP}}(X, \partial_t X)\,dt\ +\ \lambda\,\mathcal{R}[X]\ +\ \mu \int_0^T S(t)^2\,dt. \tag{117}$$

The first term enforces the native RSVP dynamics. The second enforces cross-modal reconstructibility. The third penalises entropy accumulation, preventing the system from preserving structure only by allowing indefinite uncertainty growth. The variational principle is

$$X^* = \arg\min_X \mathcal{A}[X]. \tag{118}$$

Definition 4 (Reconstructive Meaning)**.** *A structure Y has reconstructive meaning relative to a projection family $\{\mathcal{P}_k\}$ if there exists an admissible RSVP field configuration X^* such that $Y = \mathcal{P}_k(X^*)$ for some k, and X^* minimizes the reconstruction action $\mathcal{A}[X]$.*

This definition separates meaning from mere signal presence. A signal fragment may exist in one modality without being meaningful if it cannot be reconciled with the others. Conversely, a weak or partial cue may carry high meaning if it reliably reconstructs the same invariant across modalities — precisely the ecphory structure of Section 9.

Proposition 9 (Meaning as Projection-Stable Reconstruction)**.** *If X^* minimizes $\mathcal{A}[X]$, then any two admissible projections $\mathcal{P}_k(X^*)$ and $\mathcal{P}_\ell(X^*)$ are equivalent up to bounded reconstruction error. Meaning is preserved not by identity of medium but by stability of reconstruction across media.*

Hyperbionic text is one projection in this variational system. Its role is not to decorate lexical tokens but to reduce $\mathcal{R}[X]$: it makes the typographic projection more faithful to the acoustic, motor, and contextual projections of the same underlying field. Plain text has high reconstruction loss because it collapses prosody, cadence, gesture, and environmental grounding. Hyperbionic text lowers that loss by restoring enough visual structure for the reader to reconstruct the field trajectory.

The Hyperbionic rendering operator R is therefore a reconstruction-energy minimizer: it chooses visual transformations that preserve prosodic invariants while satisfying legibility constraints. The optimal rendering is not the most expressive rendering, but the one that minimizes reconstruction loss subject to perceptual admissibility:

$$R^* = \arg\min_R \left(\mathcal{R}[R] + \nu\, C[R]\right), \tag{119}$$

where $C[R]$ is the typographic constraint energy. This closes the loop between RSVP dynamics and Hyperbionic typography: both are governed by the same principle of constraint-preserving reconstruction under the variational action $\mathcal{A}$.

Spherepop Integration: Prosody as Irreversible Constraint Accumulation

---

This section situates the Hyperbionic pipeline within the Spherepop process-oriented architecture. Spherepop models computation as irreversible event history: each event is a committed, non-retractable pop that accumulates constraint. Prosodic trajectories, TARTAN tiles, and the differential prosodic envelope all have precise Spherepop interpretations that deepen the invariant-preservation account without introducing new machinery.

Trajectories as Event-Historical Traces

In Spherepop, the fundamental computational object is not a state but a history: a sequence of pops, each of which commits a constraint that cannot be undone by future events. The trajectory $\Gamma = \{Z_\alpha(t_k)\}_{k=1}^N$ has exactly this structure. Each salience packet $\mathcal{P}_k$ is an event: a peak detection that is irreversible (the peak either occurred or it did not), that commits a constraint (the inter-peak interval Δt_k and amplitude a_k are recorded as fixed values), and that is non-retractable (later packets cannot alter earlier ones, only extend the history).

The trajectory Γ is therefore not a sequence of states but a *constraint history*: a record of irreversible commitments made by the acoustic signal as it evolved. This matches the Spherepop semantics precisely. The modal coordinate $Z_\alpha(t_k) = Q(\phi(\mathcal{P}_k))$ is the Spherepop output of the k-th pop: a committed, quantized encoding of the constraints imposed by that event. Aggregation $\mathcal{M}(u) = \mathcal{A}(\{P_k\})$ is a summary functional over the history, not the history itself the distinction the paper drew between packets as fundamental and the prosodic vector as derived.

Definition 5 (Prosodic Event History)**.** *The prosodic event history of a waveform $u(t)$ is the ordered sequence*

$$\mathcal{H}(u) = (\mathcal{P}_1, \mathcal{P}_2, \ldots, \mathcal{P}_N), \tag{120}$$

where each $\mathcal{P}_k$ is a committed, irreversible constraint on the prosodic trajectory, and the trajectory Γ is the pushforward of $\mathcal{H}(u)$ under the quantization map $Q \circ \phi$.

TARTAN Tiles as Recursive Constraint Buffers

In Spherepop, complex computations are structured by layered pops: outer pops accumulate constraints over longer histories; inner pops record local events. The TARTAN hierarchy $\{\mathcal{T}_\ell(\Gamma)\}_{\ell=0}^L$ is exactly this structure.

Each tile $\tau_{\ell,j} = (\bar{Z}_{\ell,j}, \Sigma_{\ell,j}, \eta_{\ell,j}, \chi_{\ell,j}, b_{\ell,j})$ is a committed summary of the constraint history within its temporal extent. The boundary flag $b_{\ell,j}$ is a Fracture record: a committed observation that a silence or voiced-segment boundary occurred within the tile, which cannot be revised by finer-grained tiles at level $\ell + 1$ or coarser tiles at level $\ell - 1$. The propagation of $b_{\ell,j}$ up the hierarchy is therefore not interpolation or estimation it is constraint inheritance: coarser tiles inherit the irreversibility commitments of the finer tiles they summarize.

Proposition 10 (Fracture as Irreversible Commitment)**.** *A Fracture marker $b_{\ell,j} = 1$ at level ℓ is an irreversible commitment: it forecloses any reconstruction that would require aligning voiced content across the silence boundary recorded in tile (ℓ, j). This commitment is inherited by all coarser tiles that contain (ℓ, j), and cannot be revised by evidence from finer tiles.*

This is the Spherepop semantics of TARTAN: each tile pop commits a constraint on which alignments are admissible, and the DTW coherence functional (29) respects those commitments by restricting alignment paths to within connected voiced components Γ_m of the decomposition (42).

Differential Envelopes as Irreversibility Encoding

The differential prosodic envelope $\nabla p_i = p_i - p_{i-1}$ introduced in Section 20 encodes the rate of change between adjacent tokens. Its Spherepop interpretation is precise: it records the irreversibility of the transition between consecutive events.

A pitch drop from f_{i-1} to f_i is not equivalent to a pitch rise of the same magnitude in the opposite direction, even if the endpoint f_i is the same. The prosodic meaning of a descent is not the time-reversal of an ascent: falling intonation encodes finality or assertion in many languages; rising intonation encodes continuation or query. The signed gradient $\nabla f_i < 0$ versus $\nabla f_i > 0$ encodes a directional commitment that is irreversible in the Spherepop sense the history of how a pitch value was reached is semantically distinct from the value itself.

Formally, the extended parameter vector $\tilde{p}_i = (p_i, \nabla p_i)$ is an event in the event history $\mathcal{H}(u)$: it commits not only the current parameter value but the direction of arrival, which cannot be erased by subsequent values. This is why the salience-weighted rendering operator R_s in Section 20 should in principle also weight the differential components: a large signed gradient with high salience (a sharp, salient pitch drop) should render as a visually committed directional transition, not merely as a difference in endpoint values.

Reading as Constraint Accumulation

The Spherepop model of computation as constraint accumulation gives a precise account of what a reader does when encountering Hyperbionic text. Reading is not a process of decoding stored symbols. It is a process of accumulating the constraint history of the speaker's vocal intent, pop by pop, as the eye traverses the rendered trajectory.

Each Hyperbionic token $\mathcal{H}(T_i, p_i)$ is a pop in the reader's accumulation process: it commits a constraint on the prosodic trajectory that the reader is reconstructing. High-salience tokens ($s_i \approx 1$) commit strong constraints; low-salience tokens ($s_i \approx 0$) commit weak constraints that leave the trajectory under-determined at that point. The accumulated history of these commitments is the reader's internal representation of the speaker's prosodic trajectory not a symbol sequence, not a feature vector, but a Spherepop constraint history that can be used to re-enact the original acoustic event history $\mathcal{H}(u)$ within the bounds allowed by the reconstruction loss $\mathcal{R}[R]$.

A Hyperbionic document is a Spherepop program for

reconstructing a voice.

The irreversibility of this process is what gives it semantic force. A reader who has accumulated the constraint history of a falling-intonation declarative cannot simply re-read it as a rising-intonation query by reversing the differential envelope: the boundary constraints, salience weights, and coherence values committed at each pop foreclose that reinterpretation. The trajectory is directed; reading it accumulates irreversible commitments that constrain interpretation in exactly the way the speaker's acoustic event history constrained the original prosodic trajectory.

Triangular Equivalence

The full equivalence (50) has a natural geometric form. The three trajectory representations—audio, memory, and text—are not linearly ordered but mutually projectable: any two can be converted to the third via the operators defined in the preceding sections. This mutual projectability is represented in Figure 5.

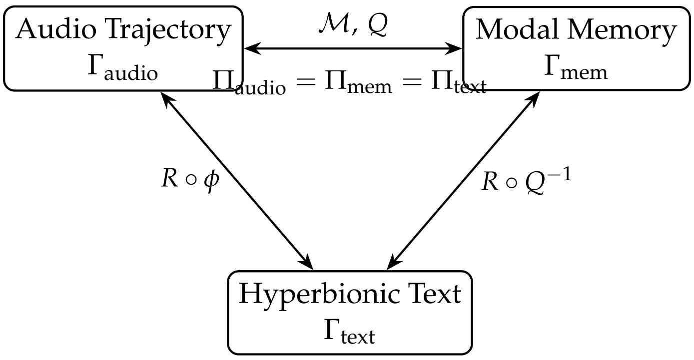

Figure 5: Triangular equivalence of the three trajectory representations. Each vertex is a representation of the same prosodic invariant structure in a different medium. The double-headed arrows indicate structure-preserving projections in both directions. The central identity states that all three projection operators extract the same invariants from their respective media.

Definition 6 (Prosodic Invariant Field)**.** *The* prosodic invariant field *is the equivalence class of all representations—audio, modal, typographic—that preserve the projection operator* Π*. Formally, it is the fiber over* Π *in the bundle of signal representations over the shared parameter space.*

The three vertices of the triangle are sections of this field over different media. The equivalence (50) holds conditionally: $\Pi_{\text{audio}}(u) = \Pi_{\text{mem}}(Z) = \Pi_{\text{text}}(R(g, p))$ if and only if the operators R and Q are *admissible* in the sense of being invariant-preserving (no distinctions present in the parameter space are collapsed) and non-collapsing (no distinctions absent from the parameter space are introduced). This makes triangular equivalence a design criterion testable by inspection of the rendering and quantization maps.

The three sides of the triangle correspond to three distinct operations. The top edge is the Marine–MEM|8 chain: acoustic measurement $\mathcal{M}$ followed by fixed-point quantization Q, converting audio trajectories into modal lattice coordinates. The left edge is the rendering chain: the projection ϕ from packet space to prosodic parameter space followed by the Hyperbionic rendering operator R, converting audio trajectories directly into visual typography. The right edge is the reconstruction chain $R \circ Q^{-1}$: reading a Hyperbionic rendering back through the inverse quantization to recover a prosodic vector, and then synthesizing an audio trajectory consistent with that vector.

The central identity $\Pi_{\text{audio}} = \Pi_{\text{mem}} = \Pi_{\text{text}}$ is the claim that all three projection operators extract the same invariant structure. This is not a tautology: it is a constraint on the design of the rendering operator R and the quantization operator Q, requiring that neither introduces distinctions not present in the prosodic parameter space and neither collapses distinctions that the other preserves. A rendering operator that maps two distinct prosodic vectors to the same visual output violates the constraint; so does a quantization scheme that conflates vectors that the rendering operator distinguishes. The triangular equivalence is therefore a testable design criterion, not merely a philosophical claim.

Categorical Structure: Functorial Projections Between Trajectory Categories

The operators $\mathcal{M}$, Q, R, and $\mathcal{P}_{\text{mim}}$ are not merely functions between representation spaces. They are structure-preserving maps between categories of trajectories, and their compositions commute up to invariant equivalence.

Define the base category **Traj** whose objects are prosodic trajectories $\Gamma \subset V = (\mathbb{R}^8, G)$ and whose morphisms are admissible transformations preserving the invariant $\mathcal{I}$. Each modality defines a subcategory:

$$\mathbf{Audio}, \quad \mathbf{Mem}, \quad \mathbf{Text}, \quad \mathbf{Motor}, \tag{121}$$

where **Audio** contains waveform-parameterized trajectories, **Mem** contains modal lattice trajectories, **Text** contains Hyperbionic typographic trajectories, and **Motor** contains mimetic gesture trajectories. The operators become functors:

$$\mathcal{M} : \mathbf{Audio} \to \mathbf{Traj}, \qquad R : \mathbf{Traj} \to \mathbf{Text}, \qquad \mathcal{P}_{\text{mim}} : \mathbf{Traj} \to \mathbf{Motor}. \tag{122}$$

The commutativity condition — that all paths between modalities yield the same invariant — is expressed as a commuting diagram over four modalities:

$$R \circ \mathcal{M} \;\simeq\; \mathcal{P}_{\text{mim}} \circ \mathcal{M}, \tag{123}$$

and analogously for all other compositions. In plain terms: whether the signal is routed audio $\to$ text, or audio $\to$ motor $\to$ text, the invariant $\mathcal{I}$ is preserved. No modality is primary; all are coordinate charts on the same underlying object.

Proposition 11 (Functorial Characterisation of Invariant Preservation)**.** *All modalities are functorial projections of* **Traj**. *A representation is admissible if and only if the corresponding functor is faithful with respect to $\mathcal{I}$: it preserves morphisms that are distinct under the invariant.*

The aggregation impossibility result (Section 18) now has a precise categorical statement: the aggregation map $\mathcal{A} : \textbf{Traj} \to \mathbb{R}^n$ is not faithful. It collapses morphisms that are distinct in **Traj**—it identifies trajectories that are geometrically different—and therefore destroys the categorical structure that carries expressive meaning. Standard acoustic embedding systems are instances of non-faithful functors; the trajectory-based architecture is an instance of a faithful one.

Multimodal Disambiguation: Contextual Grounding of Prosodic Invariants

This section addresses a structural limitation of single-modality prosodic analysis: the same invariant vector can arise from physically distinct causes. Additional modalities resolve this degeneracy not by adding information arbitrarily, but by intersecting independent constraint sets over the interpretation space.

The prosodic measurement operator $\mathcal{M}$ is many-to-one with respect to underlying causes. The same invariant vector $\mathcal{I}(u)$ can arise from physically distinct situations: elevated energy and increased jitter might correspond to anger, physical exertion, environmental noise compensation, or distance from the microphone. Formally, there exist distinct signal contexts $x_1 \neq x_2$ such that

$$\mathcal{M}(u_{x_1}) = \mathcal{M}(u_{x_2}), \tag{124}$$

where u_{x_i} denotes the acoustic waveform produced in context x_i. This degeneracy is not a failure of the measurement operator: it reflects the genuine fact that prosody is a projection of a higher-dimensional causal space onto a lower-dimensional invariant space. The invariant is real; the ambiguity lies in the inverse problem of recovering cause from invariant.

Contextual Operators and Constraint Intersection

The resolution is not to add more prosodic dimensions but to introduce a complementary *contextual operator* C that maps environmental observations into a parameter space over causes:

$$C : \text{environment} \to \mathbb{R}^m, \tag{125}$$

where the environment includes visual scene, spatial configuration, device state, and any other modality that constrains the causal interpretation. The joint invariant is then

$$\mathcal{I}_{\text{joint}} = \big(\mathcal{I}(u),\ C(\text{environment})\big), \tag{126}$$

and disambiguation is the process of finding the intersection of the prosodic and contextual constraint sets. The same prosodic vector $\mathcal{I}(u)$ combined with different contextual vectors C yields different realised interpretations: elevated energy combined with visual evidence of a distant interlocutor implies distance compensation; combined with a tense facial expression at close range, it implies anger; combined with a construction-site acoustic signature, it implies environmental override.

A photograph, markup tag, or spatial sensor is not adding a new kind of information to the system; it is providing a constraint that carves the interpretation manifold $\mathcal{I}^{-1}(\mathcal{I}(u))$—the set of all contexts that produce the observed invariant—into a smaller admissible region. The disambiguation is the intersection of the prosodic fiber with the contextual constraint set.

The Admissibility Condition on Additional Modalities

The key design principle is not that more channels are always better. Additional modalities must be co-registered with the invariant structure: they must be aligned in time, parameterized in a space that has a well-defined projection onto the causal interpretation manifold, and consistent with the admissibility constraints already imposed on the primary prosodic channel.

Misaligned markup—irrelevant images, noisy metadata, or temporally inconsistent annotations—does not reduce ambiguity; it increases entropy in the interpretation space. In the framework of this paper, this is the multimodal analogue of spectral fracturing: additional channels that impose a reconstruction burden without contributing constraint resolution degrade the system's coherence rather than improving it. The admissibility condition on additional modalities mirrors the admissibility condition on typographic rendering: the new channel must be invariant-preserving and non-collapsing with respect to the joint interpretation space.

Prosodic and Contextual Invariants

The extended framework separates two roles that single-modality analysis conflates:

$$\underbrace{\mathcal{I}(u)}_{\text{internal dynamics}} \quad \oplus \; \underbrace{C(\text{environment})}_{\text{external grounding}}. \tag{127}$$

Prosodic invariants determine the space of possible interpretations by specifying location, curvature, and coherence in the modal parameter space. Contextual invariants determine which interpretation is realised by grounding those dynamics in external causes. One gives you the geometry of the signal; the other gives you its referent.

Hyperbionic text encodes the first term of (127): it preserves the internal dynamics of the signal across modalities. Environmental markup—photographs, spatial tags, device-state annotations—encodes the second term. A fully grounded Hyperbionic document would carry both, making the interpretation space closed: the reader can recover not only the prosodic structure of the utterance but the causal context in which it was produced.

Embodied Prosody: Mimetic Proxy, ASL Classifier Dynamics, and the Motion Layer of Meaning

This section extends the invariant framework into embodied cognition. Prosodic trajectories are not merely acoustic features but motor-reconstructible structures whose loss under transcription produces systematic semantic impoverishment. The analysis draws a formal equivalence between speech prosody, mimetic simulation as theorized by Cox, and classifier dynamics in American Sign Language, establishing that Hyperbionic rendering restores an objectively real layer of meaning—not a stylistic enhancement.

Mimetic Proxy and the Motor Basis of Prosodic Meaning

Arnie Cox's theory of music cognition proposes that perceived sound is internally reconstructed as bodily motion [5]. Listeners do not merely hear a rhythmic phrase or a melodic contour: they covertly simulate the gestures that would produce or accompany it. A staccato burst evokes short, repeated motor impulses—tapping, bouncing; a sustained legato line evokes continuous smooth extension—

gliding, stretching. This *mimetic proxy* relationship means that acoustic signals are interpreted through an implicit motor mapping that is prior to, and partly constitutive of, semantic content.

Spoken language carries the same structure. Clipped speech maps to discrete motor pulses; elongated vowels map to continuous extension; rising pitch maps to upward gesture; jitter and vibrato map to oscillatory motion. Two utterances can be lexically identical but mimetically distinct, inducing divergent interpretations through the motion layer rather than the symbolic layer. A repeated, bouncing rhythmic pattern in speech can signal insistence, playfulness, or agitation; words alone do not disambiguate this. The trajectory of the signal does.

Within the present framework, this mapping is not external to the signal but inherent in its trajectory representation. Let $\Gamma = \{Z_\alpha(t_k)\}$ be a prosodic trajectory in modal space $V = (\mathbb{R}^8, G)$. We define the *mimetic projection operator*

$$\mathcal{P}_{\text{mim}} : \Gamma \longrightarrow \mathcal{G}, \tag{128}$$

where $\mathcal{G}$ is a space of motor gestures parameterized by direction, amplitude, periodicity, and continuity. The operator $\mathcal{P}_{\text{mim}}$ maps prosodic curvature and coherence into reconstructible motion primitives.

Proposition 12 (Mimetic Equivalence)**.** *For any prosodic trajectory* Γ*, there exists a motor trajectory* $\mathcal{P}_{\text{mim}}(\Gamma) \in \mathcal{G}$ *such that perception of* Γ *is mediated by covert reconstruction of* $\mathcal{P}_{\text{mim}}(\Gamma)$*, up to equivalence in curvature and coherence. Representations that collapse curvature and coherence eliminate the mimetic proxy and thereby impoverish meaning.*

Transcription as Destruction of the Mimetic Layer

Standard transcription collapses the trajectory Γ to a sequence of lexical tokens $\{T_i\}$, eliminating curvature and coherence:

$$\Gamma \longrightarrow \{T_i\}, \tag{129}$$

with no invertible mapping. The mimetic projection $\mathcal{P}_{\text{mim}}$ is therefore undefined on plain text, forcing the reader to reconstruct motion from prior experience:

$$\{T_i\} \rightarrow \text{inferred } \Gamma \rightarrow \mathcal{P}_{\text{mim}}(\Gamma). \tag{130}$$

This is the proximate source of prosodic semantic ambiguity: distinct trajectories $\Gamma_1 \neq \Gamma_2$ collapse to the same token sequence yet induce different mimetic reconstructions. The ambiguity is not resolved by lexical content but by the motion layer that transcription destroyed. A reader with a rich internal trajectory space from extensive listening can partially reconstruct the motion; a reader without that space cannot. In both cases, the text forces inference where encoding is possible.

ASL Classifier Dynamics as Proof of Existence

American Sign Language provides a system in which motion parameters are explicitly semantic, establishing beyond dispute that the motion layer of meaning can be systematically encoded and perceived [6, 7]. Classifier constructions in ASL encode semantic aspect directly through motion properties: repetition of a movement encodes iterative or ongoing action (the signed analogue of a gerund or progressive aspect); increased velocity encodes urgency or intensity; expanded spatial extent encodes scale or magnitude; path shape encodes spatial semantics; oscillatory motion encodes instability or continuity.

The structural parallel to the present framework is precise. ASL classifier semantics can be expressed as:

$$\text{meaning}_{\text{ASL}} = (\text{handshape},\ \text{motion trajectory}), \tag{131}$$

which is formally isomorphic to the semantic decomposition of Definition 2 in the prosodic domain:

$$\text{meaning}_{\text{prosodic}} = (\text{location},\ \text{curvature},\ \text{coherence}). \tag{132}$$

In both systems, the motion component is not decorative but constitutive: removing it changes the meaning, not merely the style. ASL does not lose this layer because it encodes it explicitly in a spatial-gestural medium. Spoken language contains the same layer; written language discards it.

We formalize the ASL-to-prosody correspondence as a *classifier transformation* acting on trajectories:

$$\Gamma \ \mapsto\ \Gamma' = \mathcal{C}_{\text{cls}}(\Gamma), \tag{133}$$

where $\mathcal{C}_{\text{cls}}$ applies structured modifications such as temporal tiling (repetition $\leftrightarrow$ iterative aspect), amplitude scaling (magnitude $\leftrightarrow$ intensity), and time compression (acceleration $\leftrightarrow$ urgency). Each of these transformations modifies the curvature and temporal density of Γ in a principled way, corresponding to the motion modifications of ASL classifier constructions.

Proposition 13 (Aspect Encoding via Trajectory Transformation)**.** *Semantic aspect—iterative, continuous, urgent, attenuated—is representable as a transformation on prosodic trajectory curvature and temporal density. Two utterances with identical lexical content but distinct $\mathcal{C}_{\text{cls}}$ transformations are semantically non-equivalent. Plain text collapses this distinction; Hyperbionic text preserves it.*

Hyperbionic Rendering as Mimetic Restoration

Hyperbionic text restores the mimetic layer by rendering trajectory parameters directly into visual degrees of freedom. The rendering operator R maps the prosodic trajectory to a typographic trajectory:

$$\Gamma \xrightarrow{R} \Gamma_{\text{text}} = \{p_i\}, \tag{134}$$

where p_i encodes local energy, duration, jitter, and coherence for the i-th token. The mimetic projection is then preserved across the rendering:

$$\mathcal{P}_{\text{mim}}(\Gamma) \equiv \mathcal{P}_{\text{mim}}(\Gamma_{\text{text}}). \tag{135}$$

The classifier correspondence is concrete. A bouncing or iterative prosodic pattern—high-χ oscillatory jitter at short periodicity—appears in Hyperbionic rendering as repeated typographic modulation: micro-variations in weight, spacing, or baseline that recur with the same period as the prosodic oscillation. This is the typographic gerund: iterative motion encoded as structured repetition in the visual field. A sustained, continuous prosodic pattern—low jitter, long duration, smooth energy envelope—appears as continuous spatial deformation: gradually increasing size or baseline displacement across the token sequence. A compressed, urgent pattern—high peak density, rapid energy rise—appears as condensed spacing with elevated weight. Each of these corresponds exactly to a classifier transformation $\mathcal{C}_{\text{cls}}$ in the ASL sense.

Hyperbionic text is a perceptible motion field.

Definition 7 (Embodied Semantic Field)**.** *The embodied semantic field of an utterance is the pair*

$$\mathcal{E}(\Gamma) = \big(\Gamma,\ \mathcal{P}_{\text{mim}}(\Gamma)\big), \tag{136}$$

combining trajectory geometry with its motor reconstruction. A representation is semantically complete if and only if it preserves $\mathcal{E}$.

Plain text preserves lexical identity and discards $\mathcal{E}$. Hyperbionic text preserves $\mathcal{E}$ by encoding Γ in a perceptible visual form from which $\mathcal{P}_{\text{mim}}$ can be reconstructed. It is therefore not an augmentation of text but a recovery of the embodied semantic field that phonological transcription structurally eliminates.

Semantic Disambiguation via Trajectory Visibility

The restoration of trajectory structure resolves the degeneracy identified in Section 124. Let $\Gamma_1 \neq \Gamma_2$ be two trajectories with identical lexical projections:

$$\{T_i\}(\Gamma_1) = \{T_i\}(\Gamma_2), \qquad \Gamma_{\text{text}}(\Gamma_1) \neq \Gamma_{\text{text}}(\Gamma_2). \tag{137}$$

The Hyperbionic representation preserves distinctions that plain text collapses, allowing direct perception of differences in cadence, emphasis, and mimetic character. A transcription that records not only what a speaker said but how their voice moved encodes accent, emotional register, and communicative intent as geometric properties of the rendered text rather than as metadata or stylistic annotation.

Meaning is not only what is said, but how it moves.

Persistence, Interference, and Reconstruction

This section reinterprets the pipeline operators as a selection process rather than an extraction process. Structure is not found in signals; it is stabilized across repeated projections. Components that remain coherent under multiple transforms contribute to the invariant; those that cannot be jointly reconstructed from multiple views do not. This reframing replaces the implicit notion of feature extraction with a dynamical criterion of interference-stable persistence.

Structure as Interference-Stable Content

The pipeline

$$u(t) \;\longrightarrow\; \{\mathcal{P}_k\} \;\longrightarrow\; \Gamma \tag{138}$$

is conventionally read as feature extraction: each operator reveals a latent property of the signal. This reading is incomplete. It assumes that structure is localized and static, waiting to be uncovered. In practice, meaningful structure is not given at a point; it is stabilized across transformations.

Let $\{\mathcal{P}_k\}$ be a family of projections acting on a trajectory Γ. Each projection produces a partial observation, but no single projection is authoritative. Structure emerges through agreement across projections: components that are compatible across multiple $\mathcal{P}_k$ reinforce and persist; components that are incompatible destructively cancel. We therefore reinterpret the invariant $\mathcal{I}(\Gamma)$ not as a set of extracted features but as a configuration satisfying a consistency condition:

$$\mathcal{I}(\Gamma) \sim \bigcap_k \text{Stab}(\mathcal{P}_k(\Gamma)), \tag{139}$$

where $\text{Stab}(\mathcal{P}_k(\Gamma))$ is the set of trajectory configurations stable under projection $\mathcal{P}_k$. Structure is what survives interference. This replaces "feature extraction" with a selection principle: only those aspects of Γ that remain coherent across multiple transforms contribute to $\mathcal{I}$.

This perspective retroactively clarifies the salience formula $s = 1/(1 + \overline{j_p} + \overline{j_a})$: salience is not a measure of amplitude but of cross-projection stability. A peak with high amplitude but inconsistent timing across analysis windows contributes less to $\mathcal{I}$ than a quieter peak whose temporal position is stable across the EMA projection, the period validity gate, and the harmonic coherence estimate. Salience is persistence, not energy.

Admissibility as Graded Persistence

Admissibility has previously been defined as a binary constraint: a trajectory satisfies $C[\gamma] \leq C_{\max}$ or it does not. This can be refined into a graded dynamical property.

Consider a composition chain of operators acting on Γ:

$$\Gamma \xrightarrow{\mathcal{P}_{k_1}} \mathcal{P}_{k_1}(\Gamma) \xrightarrow{\mathcal{P}_{k_2}} \cdots \xrightarrow{\mathcal{P}_{k_n}} \mathcal{P}_{k_n} \circ \cdots \circ \mathcal{P}_{k_1}(\Gamma). \tag{140}$$

A component of Γ is *persistent* if it remains reconstructible under such compositions. Define the persistence functional:

$$\Pi(\Gamma) = \int_0^T \mathbf{1}\big[\text{reconstructible at depth } t\big]\, dt, \tag{141}$$

measuring the total duration over which Γ's structure survives the operator chain. Admissibility then becomes graded: highly persistent components dominate the representation; transient components naturally attenuate without requiring explicit removal. What appears as filtering is the failure of unstable components to propagate through the chain. The constraint energy $C[\gamma]$ is a proxy for low persistence: high misalignment θ, high uncertainty S, and high vorticity ξ all correspond to components that do not survive repeated projection.

Reconstruction as the Criterion of Meaning

Let $\{\mathcal{P}_k(\Gamma)\}$ be the set of projections of a trajectory. A candidate representation $\hat{\Gamma}$ is consistent if it reproduces these projections within tolerance:

$$\mathcal{P}_k(\hat{\Gamma}) \approx \mathcal{P}_k(\Gamma) \quad \forall k. \tag{142}$$

Define the coherence supremum:

$$\mathcal{I}(\Gamma) = \sup_{\hat{\Gamma}} \operatorname{Cons}\big(\hat{\Gamma}, \{\mathcal{P}_k(\Gamma)\}\big), \tag{143}$$

where Cons measures the degree to which $\hat{\Gamma}$ satisfies (142). Meaning is identified not with what is stored but with what can be reconstructed: a structure is meaningful to the extent that it admits a stable inverse across the projection family. Components that cannot be jointly reconstructed from multiple views do not contribute to $\mathcal{I}$, and therefore do not participate in the invariant.

This reframing resolves a conceptual ambiguity that the preceding sections leave implicit. Hyperbionic text does not contain the prosodic signal in the way that a recording contains audio. It is a projection of Γ into typographic parameter space, and a reader does not decode that projection but reconstructs Γ from it using their stored trajectory space. What the Hyperbionic rendering does is shift the reconstruction burden from inference (guessing the trajectory from lexical cues alone) to perception (reading the trajectory from explicit visual parameters). The reconstruction still occurs; what changes is how much of the work is done by the rendering versus the reader's internal models.

Persistent Substrate and Rendered Observation

The distinction between persistent and transient components induces a natural architectural separation. Write

$$u(t) = X(t) + \varepsilon(t), \tag{144}$$

where $X(t)$ is the persistent substrate and $\varepsilon(t)$ is transient noise. The projections $\{\mathcal{P}_k\}$ act primarily as observation operators, producing rendered views of $X(t)$ modulated by $\varepsilon(t)$. The role of the pipeline is not to store rendered outputs but to recover $X(t)$ as the invariant structure that generates them.

In this sense, text, symbols, and all discrete outputs are not fundamental objects. They are downstream renderings of a continuously evolving substrate. Stability resides in the substrate; variability resides in the renderings. This precisely matches the triangular equivalence: audio, memory, and text are three renderings of the same $X(t)$, and the invariant $\mathcal{I}$ is the persistent substrate that all three projections share. Plain text has high reconstruction loss because it discards too much of $X(t)$; Hyperbionic text has lower reconstruction loss because it preserves more of $X(t)$'s geometric structure in its rendering.

Rendering Extensions and Field-Theoretic Connections

This section develops four concrete rendering extensions latent in the existing framework—differential prosodic envelopes, haptic field modulation, expressive coherence as a visual filter, and salience-based reconstruction cues—and establishes the precise connection between the prosodic invariant field and the RSVP constraint-energy framework.

Differential Prosodic Envelopes

The rendering operator R defined in Section 4 maps the parameter vector p_i of each token to a visual configuration. This treats tokens as isolated parameter islands. A natural extension replaces absolute parameter values with their rates of change between adjacent tokens.

Define the *differential prosodic envelope* at token T_i as

$$\nabla p_i = p_i - p_{i-1}, \tag{145}$$

and extend the parameter vector to include both value and gradient:

$$\tilde{p}_i = (p_i,\ \nabla p_i) \in \mathbb{R}^{2m}. \tag{146}$$

The extended rendering operator $\tilde{R}(g_i, \tilde{p}_i)$ then maps gradient components to visual transition properties: a rapid pitch drop ($\nabla f_i \ll 0$) produces a descending baseline shift between T_{i-1} and T_i; a sharp energy rise ($\nabla e_i \gg 0$) produces an accelerating weight transition; a sustained plateau ($\nabla p_i \approx 0$) produces stable, uniform rendering. The page becomes not a collection of styled points but a continuous visual wave whose slope encodes the kinetic structure of the speech trajectory.

This extension is motivated by the auditory system's well-documented sensitivity to contrast rather than absolute level: a sudden pitch drop is more communicative than a sustained low pitch, and a sudden onset of energy is more salient than sustained loudness. The differential envelope makes this contrast structure explicit in the visual rendering. Formally, the extended admissibility constraint is:

$$\tilde{C}[\tilde{p}] = C[p] + \mu \int_{\mathcal{M}} \|\nabla p(x)\|_G^2 \, d\mu(x) \leq C_{\max}, \tag{147}$$

where $\mu > 0$ penalises excessively rapid visual transitions that would impose a perceptual discontinuity load on the reader, analogous to pre-echo in spectrally fractured audio.

Haptic Field Modulation

The infrasound channel $H(u_{\text{infra}})$ and ultrasonic channel $H^{+}(u_{\text{ultra}})$ defined in Section 15 are both field-like in their perceptual character: they are felt across the whole body rather than localized to specific tokens. Their visual analogue should therefore be field-level rather than glyph-level.

Define the *haptic field modulation* as a global layout operator $\mathcal{F}$ that acts on the document background rather than on individual glyphs:

$$\mathcal{F}(A_{\text{lf}}, \sigma_{\text{lf}}) : \text{layout} \;\to\; \text{modulated layout}, \tag{148}$$

where the low-frequency energy envelope A_{lf} modulates a slow background oscillation in baseline grid position, margin width, or inter-line spacing, and the variance σ_{lf} modulates the depth of that oscillation. A high-energy, low-variance infrasound component (such as the sustained resonance of a large acoustic space) produces a slow, regular global field oscillation; a high-variance component (such as the irregular pulse of a crowd) produces an irregular field deformation.

Crucially, $\mathcal{F}$ must not affect individual glyph legibility: it operates at spatial frequencies far below the glyph scale, so that a reader focused on individual tokens perceives only the stable rendering $R(g_i, p_i)$, while peripheral and global perception registers the haptic field. This mirrors the psychophysical distinction between focal auditory attention (localized to specific frequencies and times) and diffuse somatic perception (distributed across the body and insensitive to rapid local variation).

Expressive Coherence as a Visual Filter

The expressive coherence χ defined in Section 15 distinguishes structured jitter (vibrato, groove, articulation) from random jitter (noise, damage, uncertainty). This distinction should be rendered visually through distinct filter modes rather than a single continuous scale.

Define two rendering filters based on (η, χ) tile classification (98):

$$\begin{aligned}
(\eta > 0,\ \chi \approx 1) \;&\Rightarrow\; \text{harmonic oscillation filter:}\\
&\quad \text{glyphs modulate with a smooth, periodic micro-variation in weight or baseline,}\\
&\quad \text{period matched to the expressive jitter frequency.} \qquad (149)\\
(\eta > 0,\ \chi \approx 0) \;&\Rightarrow\; \text{stochastic noise filter:}\\
&\quad \text{glyphs acquire a fine-grained blur or opacity scatter}\\
&\quad \text{without periodic structure.}
\end{aligned}$$

The harmonic filter is the visual gerund: structured, repetitive motion encoded as periodic typographic modulation, directly continuous with the ASL classifier dynamics of Section 17. The stochastic filter is visual noise: the reader perceives the signal as damaged or uncertain, matching the acoustic interpretation. A reader encountering the harmonic filter on a token sequence knows, without explicit annotation, that the speaker was in controlled expressive motion; encountering the stochastic filter, they know the signal was compromised. The two filters are perceptually distinct even at small modulation depths, because human visual perception is sensitive to the difference between periodic and aperiodic variation.

Salience-Based Reconstruction Cues

The ecphory connection established in Section 9 (Tulving [1]) frames Hyperbionic text as a structured cue set for prosodic reconstruction: the rendered glyph is the retrieval cue, and the reader's stored acoustic engrams supply the remainder of the reconstructed signal. This cue-based architecture implies a natural rendering principle: parameters with high salience s_i should be rendered with high visual fidelity (sharp, fully saturated transformations), while parameters with low salience should be rendered with reduced fidelity (ghosted, blurred, or attenuated transformations).

Define the *salience-weighted rendering operator*:

$$R_s(g_i, p_i) = s_i \cdot R(g_i, p_i) + (1 - s_i) \cdot R(g_i, \mathbf{0}), \tag{150}$$

where $R(g_i, \mathbf{0})$ is the default unstyled rendering. At $s_i = 1$, the full prosodic transformation is applied; at $s_i = 0$, the glyph reverts to plain text. Intermediate values produce a continuous interpolation, so that parameters below the salience threshold fade gracefully rather than switching abruptly.

This rendering principle exploits the Bayesian structure of reconstruction: high-salience parameters carry the most information about the original signal and should be rendered with the highest visual weight; low-salience parameters contribute less and should be correspondingly subdued. The reader's visual attention is drawn to the parts of the rendering that carry the most signal, and the reconstruction burden is concentrated there. A Hyperbionic rendering is not uniformly styled: it has a salience topography, and reading it follows that topography in the same way that listening follows the energy topography of the acoustic signal.

Magnitude as a Typographic Channel: The Dactyl Case

Every rendering rule considered so far attaches a physical property, size, baseline height, spacing, opacity, to a prosodic parameter extracted from an acoustic signal. A limiting case removes the acoustic signal entirely and attaches physical property directly to the symbolic value of a digit, giving a degenerate but unusually clear instance of the general principle that ordinary typography treats size and position as independent of meaning while Hyperbionic rendering does not.

Let $d \in \{0, 1, \ldots, 9\}$ be a decimal digit, and define a magnitude-bearing digit face by a size function

$$s(d_i) < s(d_j) \quad \text{whenever} \quad d_i < d_j, \tag{151}$$

with zero rendered as the limiting case, a single point rather than a full-sized glyph, so that the whole family reads as an ordered expansion away from an origin,

$$\bullet \ < \ 1 \ < \ 2 \ < \ \cdots \ < \ 9. \tag{152}$$

Ordinary numerals are nominal with respect to their own rendering: a printed 9 occupies whatever advance width the font assigns it, typically identical to every other digit's, and its magnitude has to be recovered symbolically, by recognizing which character it is, before it is available at all. A digit rendered under (151) carries its magnitude twice, once discretely in glyph identity and once continuously in physical extent,

$$d \ \longmapsto \ \Big(\underbrace{G(d)}_{\text{exact, symbolic}} , \ \underbrace{s(d)}_{\text{approximate, continuous}} \Big), \tag{153}$$

so that a viewer who has not yet identified which digit is present can already extract an approximate magnitude from its size alone, a genuinely analog read available before the genuinely digital one completes.

This is the same operation, run to its extreme, that mature Standard Galactic already performs more subtly on letters: later characters in that alphabet's own ordering were deliberately enlarged and raised, giving alphabetic position a weak continuous expression in glyph geometry, exactly the kind of auxiliary, low-spatial-frequency cue that lets a reader register a word's coarse shape before resolving its individual strokes. A digit face under (151) is what results when that auxiliary channel is made the primary one, for an alphabet, decimal digits, whose ordering is not merely conventional but genuinely numeric, so that size can track it exactly rather than approximately.

Applied to a running clock displaying hundredths of a second, the effect compounds over time as well as space. The fastest-changing place cycles through the full digit sequence many times per second, and under (151) each cycle is visually a repeated growth and collapse, $\bullet \to 1 \to \cdots \to 9 \to \bullet$, rather than a sequence of same-sized replacements. Slower positional columns, tenths, seconds, repeat the same growth-collapse cycle at correspondingly lower frequencies,

$$f_{0.01} > f_{0.1} > f_1 > f_{10} > \cdots, \tag{154}$$

so that ordinary positional carrying, invisible in conventional digital display, becomes directly visible motion: a column reaching its maximum extent, collapsing to a point, and incrementing the next-slower column by one unit. The display is closely analogous to an hourglass, which maps elapsed time onto an immediately perceptible physical quantity, the height of accumulated sand, rather than requiring the viewer to read a symbolic label; the nested-frequency clock is what results from cascading many such hourglasses together, one per positional digit, each triggering the next on overflow. It differs from an hourglass in the respect that matters for this essay: it is not purely analog. It presents the exact digital value and the continuous magnitude simultaneously, so that $G(d)$ remains available to a viewer who wants the precise reading while $s(d)$ is available to one who only wants an instantaneous sense of scale.

Ordinary typography treats geometry as independent of meaning. A digit whose size is its magnitude does not.

Connection to RSVP Constraint-Energy Minimisation

The prosodic invariant field $\mathcal{I}$ admits a connection to the RSVP (Relativistic Scalar-Vector Plenum) framework that is worth making explicit without overextending. In the RSVP framework, a field configuration Φ^* is the minimiser of a variational problem

$$\Phi^* = \arg\min_{\Phi} \int_0^T \left[\mathcal{L}(\Phi, \partial_t \Phi) + \lambda\, \mathcal{D}(\Phi(t), X(t)) \right] dt, \tag{155}$$

where $\mathcal{L}$ is the RSVP Lagrangian encoding an irreversibility constraint and $\mathcal{D}$ is a fidelity term. The constraint energy $C[\gamma]$ in equation (84) of the present paper is formally analogous: it penalises trajectories that exceed bounds on phase misalignment θ, uncertainty S, and rotational instability ξ, selecting from among all admissible trajectories the one that minimises constraint accumulation.

The precise correspondence is:

$$C[\gamma] \longleftrightarrow \int_0^T \mathcal{L}(\Phi, \partial_t \Phi)\, dt, \tag{156}$$

where the Hyperbionic admissibility constraint $C[\gamma] \leq C_{\max}$ plays the role of the RSVP irreversibility constraint enforcing that field configurations remain in the basin of dynamically stable trajectories.

Under the persistence-reconstruction interpretation of Section 21, the three RSVP field components acquire precise prosodic meanings. The scalar field $\Phi(x,t)$ becomes a density of persistence: a region of high Φ is one whose prosodic structure survives repeated projection and reconstruction. The vector field $\mathbf{v}(x,t)$ becomes a reconstruction flow: it governs how local representations must transform to remain consistent across projections, aligning partial observations so that a coherent global reconstruction remains possible. The entropy field $S(x,t)$ becomes a reconstruction admissibility measure: it quantifies the degree to which projections become mutually incompatible, acting as a barrier that limits how far persistence can propagate and where coherent structure can exist.

With these interpretations, the coupling among Φ, $\mathbf{v}$, and S can be read as an interference system operating at the prosodic level: Φ grows where reconstruction is stable; $\mathbf{v}$ transports and aligns that stability; S attenuates configurations that cannot remain coherent under repeated projection. The RSVP dynamics are not an external physical model being applied to prosody—they are the natural field theory of the persistence-reconstruction process that the Hyperbionic pipeline already instantiates. The prosodic invariant field $\mathcal{I}$ is an instance of a constraint-preserving projection over a scalar-vector plenum: it selects, from the full space of possible acoustic configurations, those trajectories that lie within the admissible region of the constraint manifold and projects them onto coordinate charts in audio, memory, and visual space.

Conclusion

The preceding sections have developed a single invariant structure expressed across three media: acoustic signal, geometric trajectory, and visual typography. Hyperbionic Reading is not an enhancement of text, and the three representations are not projections from a richer object to progressively poorer ones. **They are coordinate charts on a shared invariant field**—different parameterizations of the same underlying prosodic structure, each complete within its medium and mutually convertible through the operators $\mathcal{M}$, Q, and R. The boundary between writing and signal processing is not extended but removed: both are coordinate representations of the same invariant field. The Hyperbionic system is therefore not specific to text; it is an instance of a general class of invariant-preserving projections between media, in which each medium serves as a coordinate chart on a shared underlying field. The framework extends naturally to any medium that admits a measurement operator, a storage lattice, and a rendering projection that jointly satisfy the admissibility condition $\mathcal{I}(u) = \mathcal{I}(Z_\alpha) = \mathcal{I}(R(g, p))$. The argument developed in this essay has three levels.

At the representational level, acoustic waveforms, MEM|8 modal coordinates, and Hyperbionic typographic renderings are equivalent as parameterized projections of a shared prosodic parameter space. The equivalence is formalized by the commuting chain $\mathcal{M} \to Q \to R$ and the projection operators Π_{audio}, Π_{mem}, Π_{text}.

At the operational level, higher-dimensional acoustic features—delay and reverberation—admit precise typographic operators: delay becomes spatial displacement, reverberation becomes convolutional diffusion. The time-to-space correspondence is not an analogy; it is an isomorphism between the parameter spaces of acoustic signal processing and typographic rendering. The carrier transformation developed in Section 12 adds a second, independent axis to this correspondence: T_θ substitutes the graphemic system bearing the sequence while $\text{sem}(T_\theta X) = \text{sem}(X)$ and $H(X) = H(T_\theta X)$ hold by construction, so that decoding cost, not symbolic content, is what varies across carriers, a claim a published five-carrier rendering of a single essay makes directly checkable rather than merely plausible. The destructive dual developed in Section 15, clipping as the controlled removal of visual evidence, shows the enrichment side of this same isomorphism runs in both directions: whatever the rendering operator can add to a glyph, an erosion operator can remove, and the two share a single admissibility energy rather than requiring separate constraint systems. Carrier substitution, prosodic enrichment, and prosodic erosion are accordingly three independent operators, T_θ, $R(\cdot, p)$, C_λ, acting on disjoint degrees of freedom of the same glyph, each composable with the other two.

At the dynamical level, extending the framework to continuous speech treats spoken words as trajectories through modal space rather than as static feature vectors. The resulting trajectory resonance architecture for speech recognition is wave-native: it stores words as paths, compares paths by a time-warped coherence functional, and recognizes by resonant collapse rather than classification. The ergodic writing account extends this dynamism to production: a symbolic sequence is retrieved as a trajectory once its personal history has sampled its basin densely enough, and decomposed into finer units when it has not, unifying acoustic analysis, modal storage, Hyperbionic rendering, and speech recognition as instances of trajectory reconstruction across modalities.

The central consequence is the inclusion (19): plain text, parameterized text, and the full multimodal resonance field form a strict hierarchy of representational richness. Moving up this hierarchy does not add decoration to language; it recovers dimensions of communicative structure that plain transcription discards. Typography, extended into the Hyperbionic system, becomes a genuine carrier of prosodic information, and the boundary between writing and signal processing dissolves.

References

[1] Tulving, E. (1982). Synergistic ecphory in recall and recognition. *Canadian Journal of Psychology / Revue canadienne de psychologie*, 36(2), 130–147. `https://doi.org/10.1037/h0080641`

[2] Cabral, J., Fernandes, F. F., & Shemesh, N. (2023). Intrinsic macroscale oscillatory modes driving long range functional connectivity in female rat brains detected by ultrafast fMRI. *Nature Communications*, 14, 375. `https://doi.org/10.1038/s41467-023-36025-x`

[3] Marder, E., & Calabrese, R. L. (1996). Principles of rhythmic motor pattern generation. *Physiological Reviews*, 76(3), 687–717.

[4] Needham, T. (1997). *Visual Complex Analysis*. Oxford University Press.

[5] Cox, A. (2016). *Music and Embodied Cognition: Listening, Moving, Feeling, and Thinking*. Indiana University Press.

[6] Liddell, S. K. (2003). *Grammar, Gesture, and Meaning in American Sign Language*. Cambridge University Press.

[7] Emmorey, K. (2002). *Language, Cognition, and the Brain: Insights from Sign Language Research*. Lawrence Erlbaum Associates.

[8] Eide, D. M. (2011). *Uncovering the Logic of English: A Common-Sense Approach to Reading, Spelling, and Literacy*. Pedia Learning.